Response to Referee's Comments concerning manuscript *essd-2019-14*

Samuel Weber et al.

May 29, 2019

Dear Editor,

We thank for the constructive and positive feedback. The referees state the study as very interesting and further highlight the research as significant. However, they also identified a few minor issues which mainly concern minor language/editorial changes and a comment regarding the inclusion of technology and online data portal specific sections in this data publication. We addressed all the issues raised by the referees and briefly outline here the main revisions we made:

- We corrected all minor editorial/language issues (Reviewer #1).
- We reduced the complexity and improved the readability by shortening and streamlining the technology and data management section (Reviewer #1 and Reviewer #2). The information on the online data portal are now moved to the appendix.
- We reorganized and extended the field site description (Section 2, Reviewer #1).
- We removed duplicates and streamlined the whole text, mainly in sections 1, 2 and 3.
- We added short reviews of the main conclusions found so far based on this data set (Section 6, Reviewer #2).

In the revised manuscript we addressed all the referees comments and added in the general response one by one explanations (in blue) to the points raised by the referees. If the Editor wishes, we can publish an updated data. However, we would prefer to provide yearly updates at the beginning of a new calendar year.

With kind regards,
Samuel Weber + Jan Beutel
On behalf of all authors

Reply to comments made by Reviewer Paolo Pogliotti

We thank Referee Paolo Pogliotti for the review and suggestions for improvement. The response by the authors to the reviewer comments are listed and explained.

General comment: The dataset presented is impressive and of very high quality. I believe the article is excellent for publication in ESSD after a careful reorganization of the contents to make it much leaner and exclusively focused on the Pangaea dataset.

This manuscript presents an impressive dataset recorded over ten years on the north east ridge of Matterhorn, in steep bedrock permafrost conditions. The dataset includes multi-spot measures of rock temperature and resistivity at different depths, fracture kinematics, displacement and tilting of rock buttresses, time-lapse images and in situ meteorological data.Data collection methods and sensors setup are exhaustively discussed. The dataset, that includes raw data and post-processed products, is openly accessible and available from a long-term data repository (Pangaea).

The dataset is new and extremely relevant for researchers studying the instability processes related to permafrost degradation in high-mountain environment. The variety of measures represents a great added value that allows the use of these data for developing, calibrating or validating process-oriented models as well as designing and testing of remote early-warning systems. Moreover a number of specific fields of research like e.g. geomatics, hydrology, data-science and more could potentially benefit of this dataset.

To conclude, I believe the article is excellent for publication in ESSD after a careful reorganization of the contents to make it much leaner and exclusively focused on the Pangaea dataset.

Major comment 1: The manuscript provides all the informations needed to other researchers for an effective use of the dataset but sometimes these informations are lost in the complexity of the paper. This happens because the article is not exclusively focused on the dataset published in Pangaea but also on the Permasense web portal. Although the two objects are intimately linked, I believe it is important to keep them separate to promote the use of published data (that can be cited by others) rather than the use of real-time ones (that cannot). I strongly suggest moving all content related to access and use of the Permasense web portal, included the processing code published on zenodo, to appendix A or publishing it in a separate article.
Reply: We thank the referee for this comment. We agree, the manuscripts contains a lot of information and is very dense. Nevertheless, these information including complex information as for example the time synchronization are a prerequisite for full reproducibility and understanding of the data and their quality at the raw data level (which we agree is a special use case that not many people will likely be using). Further, we decided not to focus exclusively on a static data data set (e.g. the current Pangaea version) as the experiment/data acquisition at the Matterhorn Hörnligrat field site are ongoing and all the processing steps and tools are needed for a future update of the data set. Apart from future updates to the dataset by the authors the reader can update the dataset at his discretion using the toolset provided (living data process). We implemented the following changes to improve the readability: (i) removal of duplicate and confusing parts, (ii) description of the online portal in the appendix only, (iii) a clearer distinction between primary data, secondary data and the processing toolset.

Major comment 2: The Chapter 3 Technology is out of the purpose of this paper because of tailored on the hardware and software architecture of the GSN and the related storage infrastructure. These aspects are very important and impressive but, in fact, irrelevant for the effective use of the dataset. Also for this, I strongly suggest moving this chapter in appendix A or use it as core for a separate publication in another journal and keep in this publication just the essential (like e.g. figures 2 and 3).

Reply: We agree that for the downsampled derived data set in this paper, most of the technology description is not of primary importance. However to be able to understand in full and have transparency and reproducibility as well as in order to be able to leverage the high rate raw primary data set (should that be an objective) it is quite important to know details about the digitizing system and time abstraction used as the instruments used here are not commercial off the shelf (with the then available vendor documentation). It would be possible to move parts of section 3 to the appendix, but at least sections 3.2 and 3.3 on sensor integration, and large parts of section 3.4 data management would be required in the core part of the paper in order to describe the sensor/data specific aspects.
We have therefore opted to move the online access to the appendix but only streamline the sensor technology and data management section.

Major comment 3: In the context of environmental science and notably in permafrost studies, the site description (chapter 2) is important and should provide the reader (who does not know the area) with all the basic information, to frame the area in therms of climate, topography, morphology and geology. In my opinion these general informations are totally missing in the manuscript and this gap must be filled. I strongly suggest to provide the following general informations:- climate: temperature, precipitation, seasonal extremes, etc... on average-topography/morphology: mean orientation of the ridge, mean aspect and slopes of the ridge flanks,elevation interval, etc...- geology: main lithologies and rough structural setting (e.g. orientation of the main faults and fractures families...) I guess that in Haslers papers and PhD thesis all these infos are more or less ready to go. See also the technical corrections for further comments.
Reply: We fully agree and therefore added the missing information as suggested.

Major comment 4: Downloading the dataset from Pangaea repository I noticed that all the .csv files contains a lot of decimal places. In my opinion the dimension of the archives could be significantly reduced by rounding all the double values to the 2nd decimal place. Please consider this.
Reply: For some of the derived data this is possible, but for some others, e.g. crackmeters or GNSS strictly rounding to two decimal places would result in reduced fidelity/accuracy of the data. Therefore we suggest to not change this as it would generate inconsistencies in data formatting. E.g.

```
e           n           h        sd_e    sd_n    sd_h
2617909.635 1092124.515 3538.041 0.00011 0.00013 0.00027
```

Minor comment 1 (P2/R19-21): remake this sentence the sense is understandable but not easy readable. Maybe the brackets are not well positioned?
Reply: We rephrased this sentence in the revised manuscript

Minor comment 2 (P2/R24): put a comma after setting
Reply: Done.

Minor comment 3 (P2/R25): "data: The longest" uppercase after the colon. This is systematic in your paper but Mr. Google told me that is not usual: *'Capitalization: First Word After a Colon. In British English, the first letter after a colon is capitalized only if it's a proper noun or an acronym; in American English, the first word after a colon is sometimes capitalized if it begins a complete sentence'.*
Reply: Changed according the suggestion in the revised manuscript.

Minor comment 4 (P2/R25): remove the acronym w.r.t. whole over the paper (lot of occurrences), use the full words instead
Reply: Done.

Minor comment 5 (P2/R31-32): this sentence is a kind of repetition, can be removed
Reply: Removed.

Minor comment 6 (P3/R9): what do you mean with sensor (type) extension?
Reply: This section as been removed and consolidated as outlined for major comment 1 and 2.

Minor comment 7 (P3/R21-32:): move & merge this block of text in the research interest-paragraph 2.1.See also major comments n.3
Reply: Done. Section 2 has been consolidated.

Minor comment 8 (P4/R4): please provide a most statistically significant MAAT, at least over the period 2008-2018. If possible provide also the mean annual precipitation (mm), seasonal extremes and other useful climatic informations. See also major comments n.3
Reply: Done. Since the weather station has experienced serious data gaps and was only installed mid through the whole monitoring period it is not so straightforward to calculate a correct MAAT from our data. Therefore we have given one derived from literature and an example value for a period where full data from our instruments exist.

Minor comment 9 (P5/R22-25): 'All the ... context', already said at the end of the Chapter 1-Introduction... remove or merge there.
Reply: This has been removed here, the end of the intro was reformulated.

Minor comment 10 (P6-P11): See major comments n.1&2
Reply: This sentence has been shortened to only contain the sensors/features that are part of this dataset/paper.

Minor comment 11 (P12/R16-18): a description of section 5 is not pertinent here. Move it to the end of the chapter 1 or delete.
Reply: In our opinion, this statement is important to remind the reader that the derived data product is described in the next section. We moved the details to the end of the introduction as suggested.

Minor comment 12 (P12/R19): It would be very useful to have the figure 16 in this chapter, between table 2 and figure 6. This is important especially for the comprehension of caption in table 2 and remarks in rows 19-26.
Reply: Done.

Minor comment 13 (P12/R20): 'reliability in place of 'availability'
Reply: Done.

Minor comment 14 (P12/R23-24): 'Therefore... paper' is not necessary. This remark already rise up from previous sentences.
Reply: Removed.

Minor comment 15 (P12/R28-32): Remove the first sentence that is well-known and move this block at the end of paragraph. That is, start the paragraph with 'Since 2010...'
Reply: This paragraph was moved to a separate subsection in section 4.8 further data and related work.

Minor comment 16 (P13/R1): in Table 1 WXT520/536 is cited, while in text just WXT520. In fact WXT536 appears just in tab.1. Please fix this inconsistency or explain it.
Reply: The WXT536 is an updated variant of the WXT520 product. It delivers the same data although some technical (interface) details differ. We removed the reference to WXT536.

Minor comment 17 (P15/R7): define near surface in therms of depth... 10cm?
Reply: We defined *near-surface temperature* as measurement at $3-8\,\mathrm{cm}$ depth.

Minor comment 18 (P15/R8): explain the acronym NTC
Reply: Done.

Minor comment 19 (P15/R12): please, add a reference to Tab.1 after 'used'
Reply: Done.

Minor comment 20 (P15/R12): remove the last sentence, it is a repetition of row P15/R8-9
Reply: Done.

Minor comment 21 (P16/Fig.7): this figure is not cited in text (notably paragraph 4.1). Anyway I guess it is not very relevant, I let you decide whether to keep it or take it off
Reply: We changed the manuscript accordingly and now refer to the figure in the revised manuscript.

Minor comment 22 (P16/R4): explain acronym ADC. Please add the drift values also for this sensor (if possible)
Reply: ADC is corrected. The manufacturer does not supply drift information.

Minor comment 23 (P16/R10): Table 2 shows the depths of temperature measures in rock face and fractures but the indication of which of the 4 thermistor systems is used is missing.To address this task you can label (as e.g. A,B,C,D) the ground temperature in Tab.1 (first column) and text in this paragraph (P16/R1-9), then call the same labels in the caption of Tab.2 like e.g.: ^{a}Intervention: Change of thermistor system from A to D. ^{b}Intervention: Change of thermistor system from B to C. etc... Tab.2 might become little more complex but more exhaustive and meaningful.
Reply: Done.

Minor comment 24 (P17/Fig.8 and 9): due to the length of the time series, evaluate of enlarging the plots exploiting the entire width of the page while keeping fix the present height
Reply: We addressed this comment in the revised manuscript and changed Figure 7 to Figure 10 accordingly.

Minor comment 25 (P19/Fig.10): same as above
Reply: Done. See reply to minor comment 24.

Minor comment 26 (P19/R2): bis → is. This sentence could be replicated in the tables caption.
Reply: Done.

Minor comment 27 (P19/R4): remove 'here'
Reply: Done.

Minor comment 28 (P19/R6): add a comma after 'rockfall'
Reply: Done.

Minor comment 29 (P19/R13): remove the last 'remotely'
Reply: Done.

Minor comment 30 (P19/R14): comma after 'active'
Reply: Done.

Minor comment 31 (P20/R2–4): please, indicate clearly in the first sentence that what you call the primary antenna, works as a master station with respect to the others and that it is

located at point MH42/HOGR. At first glance, it was not easy to be sure of that. I know this will be discussed further in section 5.2, but it is better to have it here too.
Reply: Done.

Minor comment 32 (P22/R17-18): check the English, the sentence sounds strange
Reply: This section has been reworded in accordance with major comments 1 and 2.

Minor comment 33 (P22/R22-23): This sentence can be omitted
Reply: Minor rewording done for clarity.

Minor comment 34 (P30/R24): use acoustic emission / microseismic instead of AE/MS
Reply: Done.

Minor comment 35 (P31/R1): See major comments n. 1 & 2
Reply: Done.

Minor comment 36 (P32/Table A1): The reference to this table is missing in the text.
Reply: Done.

Reply to comments made by Anonymous Reviewer #2

We thank Anonymous Referee #2 for the review and suggestions for improvement. The response by the authors to the reviewer comments are listed and explained.

General comment: This is very excellent manuscript since it showcases comprehensive and state-of-the-arts data sets recording thermal, hydraulic and kinematic dynamics of permafrost underlying alpine bedrock cliffs where few observations have been conducted in the world due to its harsh environments. Manuscript is also written very well with perfect information of technological and geographical settings, and data quality, accordingly I strongly recommend it to be published ESSD after minor revisions.

There are two points that I would like to comment for further revisions.

Major comment 1: '6. Example of data use': In this section, the authors only listed some publications (phD thesis,etc.,) based on this data sets. I recommend to describe here more scientifically, e.g.,what was new scientific findings from simultaneous monitoring of rock fracture with AE, GNSS, resistivity, temperature and meteorological measurements? Such comprehensive monitoring is absolutely impossible in another mountains. Short reviews would be useful for the readers working out of Alps.
Reply: Done. We included more context here.

Major comment 2: The manuscript length would be shorten. There are some redundant writing in the manuscript, for instance, early parts of 2.1 Research interest at this site, it would be merged with "2. Site description". Please check more for other parts, too.
Reply: We have substantially streamlined sections 1, 2 and 3 and removed duplicate discussions in various other part. See also the answers to the major comments of reviewer one.

A decade of detailed observations (2008–2018) in steep bedrock permafrost at Matterhorn Hörnligrat (Zermatt, CH)

Samuel Weber[1,2], Jan Beutel[1], Reto Da Forno[1], Alain Geiger[4], Stephan Gruber[5], Tonio Gsell[1], Andreas Hasler[6], Matthias Keller[1], Roman Lim[1], Philippe Limpach[4], Matthias Meyer[1], Igor Talzi[7], Lothar Thiele[1], Christian Tschudin[7], Andreas Vieli[3], Daniel Vonder Mühll[8], and Mustafa Yücel[1]

[1]Computer Engineering and Networks Laboratory, ETH Zurich, Switzerland
[2]Chair of Landslide Research, Technical University of Munich, Germany
[3]Department of Geography, University of Zurich, Switzerland
[4]Institute of Geodesy and Photogrammetry, ETH Zurich, Switzerland
[5]Carleton University, Ottawa, Canada
[6]SensAlpin GmbH, Davos, Switzerland
[7]Computer Science Department, University of Basel, Switzerland
[8]SystemsX.ch Management Office, ETH Zurich, Switzerland

Correspondence: Samuel Weber (weber.samuel@tum.de)

Abstract. The PermaSense project is an ongoing interdisciplinary effort between geo-science and engineering disciplines and started in 2006 with the goals to ~~make observations possible~~ realize observations that previously have not been possible. Specifically, the aims are to obtain measurements ~~data~~ in unprecedented quantity and quality based on technological advances. This paper describes a unique ten+ year data record obtained from in-situ measurements in steep bedrock permafrost in an Alpine environment on the Matterhorn Hörnligrat, Zermatt Switzerland at 3500 m a.s.l.. Through the utilization of state-of-the-art wireless sensor technology it was possible to obtain more data of higher quality, make this data available in near real-time and tightly monitor and control the running experiments. This data set (DOI: doi.pangaea.de/10.1594/PANGAEA.897640, Weber et al., 2019) constitutes the longest, densest and most diverse data record in the history of mountain permafrost research worldwide with 17 different sensor types used at 29 distinct sensor locations consisting of over 114.5 million data points captured over a period of ten+ years. By documenting and sharing this data in this form we contribute to making our past research reproducible and facilitate future research based on this data e.g. in the area of analysis methodology, comparative studies, assessment of change in the environment, natural hazard warning and the development of process models. Finally, the cross-validation of four different data types clearly indicates the dominance of thawing-related kinematics.

1 Introduction

The behavior of frozen rock masses in steep bedrock permafrost rock slopes is a dominant factor influencing slope stability when permafrost warms or thaws (Fischer et al., 2006; Ravanel and Deline, 2014). Ongoing degradation of mountain permafrost coincides with observations of increasing rockfall activity (Ravanel and Deline, 2011; Huggel et al., 2012; Gobiet et al., 2014) potentially triggering large scale hazard events via complex process chains (Huggel et al., 2005; Westoby et al., 2014; Haeberli et al., 2017). While the long-term trend of rising permafrost temperatures can ~~be clearly~~ clearly be observed at a global scale (Biskaborn et al., 2019) warming trends of mountain permafrost are more diverse in their behavior (Noetzli et al., 2018). For example it has been recently observed that ~~a general~~ the generally warming trend can be temporarily interrupted ~~e.g. in debris slopes and rock glaciers (??).~~ depending on the amount and temporal extent of the snow cover (Noetzli et al., 2019) which is especially variable in mountainous terrain.

Numerous studies investigated the thermal and mechanical properties of frozen rock ~~as well as their relations (e.g. Mellor, 1973; Davies e~~ (e.g. Mellor, 1973; Davies et al., 2001; Gruber et al., 2003; Sass, 2004; Gruber et al., 2004b; Sass, 2005; Krautblatter and Hauck, 2007; C with the goal of furthering our understanding of the ~~acting processes~~ processes acting in bedrock permafrost in the short- and long-term (e.g. Walder and Hallet, 1985; Wegmann, 1998; Hall et al., 2002; Murton et al., 2006; Matsuoka and Murton, 2008; Hasler et al., 2011a; Girard et al., 2013; Draebing et al., 2017). ~~Many research projects~~ Several studies highlighted the relevance of dense, diverse and long-term monitoring (Hasler et al., 2011b, 2012; Weber et al., 2017) in order to mitigate effects of temporal (annual) variability and other measurement artifacts (outliers) with negative impacts on data quality and therefore potentially leading to misinterpretation (Weber et al., 2018c, b).

The Matterhorn Hörnligrat field site located in Zermatt, Switzerland at 3500 m a.s.l. is a unique situation for steep bedrock permafrost research as it is located on a ridge and not on a mountain top or in a large rock face where permafrost boreholes would typically be placed (Luethi and Phillips, 2016). A comprehensive multi-sensor setup has enabled research on surface processes and kinematics in steep bedrock permafrost in the context of environmental forcing (ambient meteorological conditions, snow cover, heat flux) since 2006. ~~All instrumentation is integrated into a low-power wireless sensor network (WSN) allowing near real-time data access. In doing so it is not only possible to monitor sensor operation and access data online, but also to control the experiments from remote, e.g. parameters can be configured according to measurement needs or selected components can be shut down at times when power is scarce in order to maximize overall data yield. Furthermore, using distributed wireless sensors (Beutel et al., 2009) significantly reduces the need for cabling and dependencies from monolithic centralized units resulting (always a single point of failure) and therefore less impact of failures of a single device on the overall system. Our experience over the past decade+ shows, that using a WSN is a promising approach with superb data availability and data quality. The sensor nodes have been running reliable and autonomous on the order of years in an extremely challenging environment and off-season/unplanned maintenance efforts are seldom necessary.~~

Situated in a ~~superbly~~ unique and iconic setting, the Matterhorn Hörnligrat field site now provides over a decade of ~~one-of-a-kind~~ mountain permafrost data: ~~The longest~~the longest, densest and most diverse data record ~~w.r.t~~ with respect to permanent monitoring of mountain permafrost at high elevation worldwide. Apart from duration and location, this data set is ~~groundbreaking w.r.t.~~ novel with respect to the diversity of the instruments used (17 different sensor types are contained in this paper), the density of the measurements both spatially (sensors are installed at 29 distinct sensor locations each containing one or more sensor ~~modalities,~~ types (see Table 2) and temporally (sampling rates on the order of per-minute to per-second)~~and the possibility to interact with the field site in near real-time in order to monitor, inspect, adapt and control the sensor systems according to specific instrumentation needs. This manuscript documents and publishes a decade of data measured at this unprecedented field site using a multitude of different sensor types in order to document and preserve this data backing up~~

~~existing and facilitating future research. ~~. The data set presented amounts to 83.8 GB of data in 41'031 files of different formats containing approximately 114.4×10^6 data points of primary and aggregated data (see Table 6). To the best of our knowledge, in the entire European Alps only the Aiguille du Midi site (Chamonix, France, 3842 m a.s.l.) ~~(Magnin et al., 2015)~~ (Ravanel and Deline, 2011; Magnin et al., 2015), the permafrost borehole on Jungfraujoch (Grindelwald, Switzerland, 3700 m a.s.l.) ~~(?)~~ (Wegmann, 1997, 1998; Noetzli et al., 2019), the geothermal profiles on Stockhorn (Gruber et al., 2004c) and two simple ground surface temperature sensors located on the summit of Matterhorn (4478 m a.s.l.) are located in comparable or at higher altitude and are being operated in a long-term monitoring mode albeit the data records are ~~much~~ shorter and offer less diversity ~~w.r.t.~~ with respect to the measurements. Other study sites at very high altitude exist, e.g. Grandes Jorasses (Chamonix, France, 4208 m a.s.l.) (Faillettaz et al., 2016) but have only been operated for a short ~~time~~ period and in campaign mode. Outside of the European Alps, mountain permafrost data is very sparse (even in the Himalaya, Gruber et al., 2017) and in cases where ground-based measurements exist they are likely limited to a single sensor type only (Zhao et al., 2010; Popescu, 2018; Gruber et al., 2015).

~~Care has been taken that all data collected are structured and stored in a coordinated fashion allowing reproducible research results and re-use of data in different contexts and in future projects. Also flexibility w.r.t. sensor (type) extension, support of different data rates, metadata integration and life-cycle management were identified as key requirements. For this purpose an online data processing and data management framework has been designed and successively extended based on a streaming data management middleware (Aberer et al., 2006).~~

~~This manuscript provides~~ This manuscript documents the complete raw data at full sampling rates of the instruments used (primary data set, see Section 3) for the most significant sensor channels/types deployed (as outlined in Section 4) as well as a selection of derived data products (~~aggregation according industry standard and common practice), code for accessing and processing this data and the respective documentation~~ secondary data set). The derived data products are downsampled and cleaned time series of the weather station, ground temperature, electrical resistivity of rock, fracture displacement and inclinometer data as well as GNSS daily positions computed using double differencing techniques. In order to be able to fully understand and leverage the high-fidelity sensor and to allow full transparency and reproducibility a technology excerpt as well as the procedures for compiling and validating the primary and secondary data sets are presented in Section ~~5. Beyond the repositories for code and data indicated~~ 3 and Section 5 respectively. Using the toolset described in Section 7 ~~the data of this publication can also be accessed on the publicly available web frontend~~ these data sets can be recreated and independently updated (living data process). The online data portal at http://data.permasense.ch (see ~~Fig.~~Figure **??**) ~~. Periodic (annual) updates~~ is discussed in Appendix **??**. In addition, select examples of the data ~~set described are planned, but using the toolset described~~ as well as an overview of the scientific results based on data from this field site are discussed in Section ~~7 and the Appendix **??** and **??** these can additionally be retrieved independently~~6.

2 ~~Site descriptionThe Matterhorn~~ Matterhorn Hörnligrat ~~field site is located on the northeast ridge of the Matterhorn in Valais, Switzerland, close to the Italian border at an elevation of 3500 m a.s.l. (white arrow in Fig. 1a, CH1903+ 617950/92168). It~~ field site

The Matterhorn is prominently known due to ~~the archetypical formof the Matterhorn mountain~~its archetypical form, the famous climbing route up the Hörnligrat ridge (northeast ridge of Matterhorn) and its dramatic first ascent on July 14, ~~1865 but also for frequent rockfall occurring with the most significant event occurring on July 15, 2003 with a volume of approximately 1500 m^3 exposing bare ice at the surface of the scarp (see red arrows in Fig. 1b and c) (Haeberli et al., 2015). Although insignificant within the scale of a mountain the age and size of the Matterhorn this particular incident showed significant susceptibility on the human scale to the processes at hand: As this rockfall event occurred in the middle of the summer climbing season and right on the popular climbing route to the summit it lead to the evacuation of 84 climbers by helicopter, the temporary closure of the climbing route and other mitigation measures being initiated (Haeberli et al., 2015). With regards to the research aspects it is this hazard event, the expectation that further (catastrophic) dynamics would likely follow and the presence of compact ice observed in the detachment zone after the rockfall event took place that lead to the selection and instrumentation of the first experiments investigating kinematics of strongly fractured, steep bedrock permafrost in the years 2006-2007 (Hasler et al., 2008). Despite its remoteness and exposure this field site is actually readily accessible being situated directly on and in the bottom segment of the climbing route with further infrastructure nearby (mountain hut, heliport, transportation facilities, Internet connectivity) and therefore can be accessed even in a day trip fashion from Zurich should that be required.~~

~~Matterhorn Hörnligrat field site is located on the North-East ridge of the Matterhorn on 3500 m a.s.l. (b) and (c) show the detachment zone after the rockfall event in July 2003 with a volume of approximately 1000 − 2000 m^3. The comparison between (c) and the detail (d) taken 2-5 days before the rockfall event indicates that the top of the ridge was almost not affected by the failure event. Photos: PermaSense, Bruno Jelk and Kurt Lauber.~~

~~This field site consists of spatially heterogeneous steep, fractured bedrock with partially debris covered ledges in discontinuous permafrost. The mean annual air temperature is −3.7 °C for the time period 2011–2012. The precipitation mostly falls as snow with rainfall events as well as occasionally snowfall, snow/rain mix during summer. Winter temperatures down to −27 °C in combination with exposure to strong wind (to over 100 km/h) results in a preferential snow deposition in fractures, on ledges and at other concave microtopographical features. On the south side the accumulated firn disappears completely during summer, while on the north side snow patches persist at this altitude all year round.~~

2.1 ~~Research interests at this site~~

~~The perfect free-standing and over-steepened pyramid of the Matterhorn has been a continuous source of fascination throughout history attracting explorers with serious goals as well as mythical story-tellers. The~~ 1865. This first successful alpine conquests on the Matterhorn ~~in 1865~~ were actually undertaken by researchers: ~~First~~ first ascent led by Edward Whymper, a writer and landscape illustrator on assignment from an English ~~publisher~~ publishing house as well as subsequently the second ascent by John Tyndall, a prominent multidisciplinary scientist of his time both accompanied by local guides and other companions. ~~Triggered by the rockfall events observed in~~ Nowadays, several hundreds to few thousands of mountaineers climb the Matterhorn via the Hörnligrat every year.

In the exceptionally warm summer of 2003 ~~(the July 15, 2003 event on the Hörnligrat ridge was not the only one, but similar rockfall was also observed on the south-west ridge of the Matterhorn (Haeberli et al., 2015) and elsewhere~~ increased rockfall activity was observed in the entire Alps (Gruber et al., 2004a; Ravanel et al., 2017)~~and an increased~~. An increasing interest into the thermal behavior of permafrost in steep topographies in these years~~(?Gruber et al., 2004c)~~ (Gruber et al., 2004b, c) lead to a first simplified modelling study based on the Matterhorn (Noetzli et al., 2007). It soon became clear that such work would require substantial evidence from long-term, in-situ measurements to calibrate and validate such models accordingly as no other comparable ~~dataset~~ data set existed. Additionally, the prominent rockfall activity observed motivated further research questions ~~w.r.t.~~ with respect to slope/rock wall stability, natural hazards (mitigation) and the susceptibility of nearby human infrastructure and urban environments to such hazards ~~(Fort et al., 2009; Ravanel et al., 2017, 2010).~~ (Gruber and Haeberli, 2007; Fort et al., 2009; Ravanel et al., 2017, 2010).

On July 15, 2003 a single rock volume of approximately $1500\,\mathrm{m}^3$ released from the Hörnligrat at $3500\,\mathrm{m}$ a.s.l. (white arrow in Figure 1a, CH1903+ 617950/92168) uncovering bare ice in the failure plan (see red arrows in Figure 1b and c) (Hasler et al., 2012). Although insignificant on the scale of a mountain the age and size of the Matterhorn as a whole, this particular incident showed significant susceptibility on the human scale to the processes governing such rockfall: As this rockfall event occurred in the middle of the summer climbing season and directly affected the popular climbing route to the summit, it led to the evacuation of 84 climbers by helicopter, the temporary closure of the climbing route and other mitigation measures (Haeberli et al., 2015). Compact ice was observed on the surface of the detachment scar right after the rockfall event suggesting clefts be filled with ice. With respect to the research aspects it is this hazard event, the expectation that further (catastrophic) dynamics would likely follow and the significant ice infill that led to the selection and instrumentation of the first experiments investigating kinematics of strongly fractured, steep bedrock permafrost in the years 2006-2007 at the Matterhorn Hörnligrat field site (Hasler et al., 2008).

Therefore an initial interdisciplinary project between geo-science and engineering was proposed with the initial goals to ~~make observations possible~~ enable observations that previously have not been possible: ~~The~~ the PermaSense project specifically aimed at (i) obtaining in-situ measurements with unprecedented quality and quantity (~~w.r.t.~~ with respect to both spatial and temporal resolution and duration) but also (ii) to try to leverage then-emerging wireless sensor network technology (Talzi et al., 2007; Hasler et al., 2008) at scale and in a real case study. The Swiss Science Foundation (SNSF) funded National Competence Center on Mobile Information and Communication Systems (NCCR-MICS Aberer et al., 2007) as well as select government funding through the Swiss Federal Office of the Environment (FOEN) supported this initial push that over time development into a ~~full fledged~~ comprehensive outdoor infrastructure and mountain lab supporting diverse experiments~~and~~ , long-term monitoring ~~. All the datafrom these efforts is available in the public domain on this web frontend:~~and online data: http://data.permasense.ch. ~~After completing the first ten years since the first experiment went live in July 2008 it's now~~

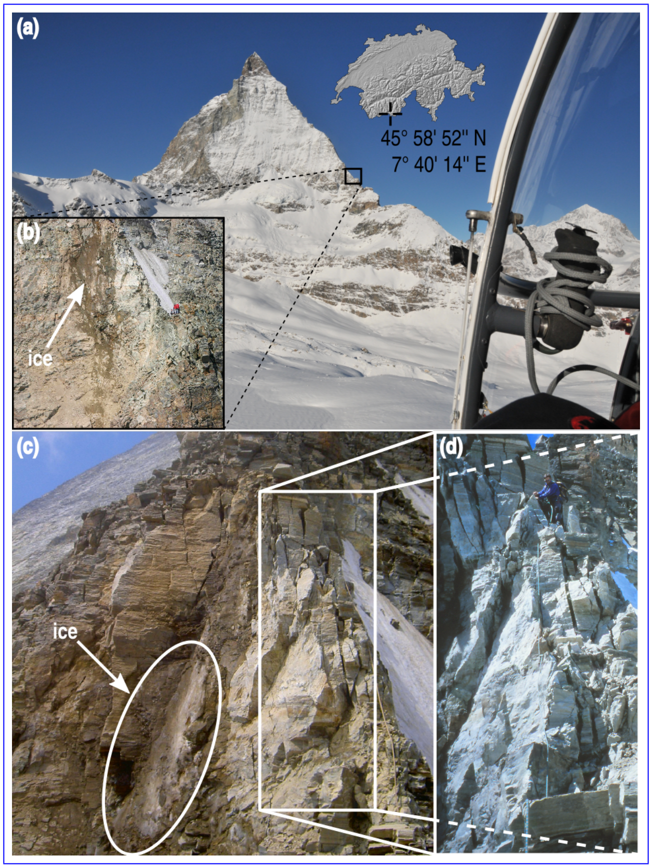

Figure 1. Matterhorn Hörnligrat field site is located on the North-East ridge of the Matterhorn on 3500 m a.s.l. (b) and (c) show the detachment zone after the rockfall event in July 2003 with a volume of approximately $1000 - 2000\,\mathrm{m}^3$. The comparison between (c) and the detail (d) taken 2-5 days before the rockfall event indicates that the top of the ridge was almost not affected by the failure event. Photos: PermaSense, Bruno Jelk and Kurt Lauber.

~~time to publish a first digest of this data including a thorough documentation in order to (i) preserve this data and (ii) make it available for future research in the broader context. The data presented in this publication constitutes a best-of of~~

The Hörnligrat field site is located at 3500 m on the North-East ridge of Matterhorn covering the area around the detachment zone of the ~~most relevant and descriptive geo-science related data collected. There are further data available in the context of this work, that either (i) have been published elsewhere (Weber et al., 2018a; Meyer et al., 2018), (ii) is not deemed suitable for publication in the context of this publication (either out of scope or to complex or too poor in quality) and (iii) have been collected by related activities in the vicinity of this field site . The most relevant of these additional data sources are described in brief in Section 4.8 in order to give the reader the relevant pointers in this context~~2003 rockfall event and consists of steep, highly fractured rock slopes with partially debris covered ledges and different expositions, where the expected occurrence of permafrost varies with aspect and relief conditions (see Figure 3 in Weber et al., 2017). Geologically, this field site consists of gneiss and amphibolite of the Dent Blanche nappe (Bucher et al., 2004) and the most dominant fractures are oriented parallel to the ridge and dip nearly vertical (see Figure 2 in Hasler et al., 2012). Climatically, the region of Zermatt is characterized by a dry and subcontinental climate with high daily/seasonal temperature fluctuations and with mean annual air temperature (MAAT) of 3.5 °C (1961–1990) and 4.2 °C (1981–1990) (MeteoSwiss, 2019). While reanalysis data with a 1x1 km^2 grid indicate a regional MAAT of −6.7 °C (1961-1990, Hiebl et al., 2009) for the field site area, local measurements at the field site show a mean annual air temperature of −3.7 °C (period 2011–2012, Weber et al., 2017). As precipitation mostly falls as snow with occasional infrequent rainfall events in summer, liquid water is mainly supplied to the site by snow melt (Hasler et al., 2012). Winter temperatures down to −27 °C in combination with exposure to strong wind (to over 100 km/h) results in a preferential snow deposition in fractures, on ledges and at other concave microtopographical features. While the northern side contains small ice field within a steep heterogeneous rock face, on the south side snow patches develop during winter in couloirs as well as on rock bands and disappear in spring/summer completely (Hasler et al., 2012).

2.1 ~~History of on-site research activities~~

Surveying and site selection took place in the years 2006/2007 with an initial sensor installation campaign in fall 2007 (Hasler et al., 2008). The technological developments started with data logger prototypes (Talzi et al., 2007) that were used for a first data retrieval campaign during ~~that~~ the following winter season. The prototype development and initial experience resulted in a redesign of the wireless sensing platform ~~(Beutel et al., 2009)~~ that was deployed for the first time on July 25, ~~2008.~~ 2008 (Beutel et al., 2009). This date also marked the start of the "production" data generation for the ~~original~~ PermaSense project and the data contained in this publication. Later technological milestones include the introduction of the GSN data management system~~later in that year~~, a switch from 3G cellular connectivity to IEEE 802.11a 5 GHz WLAN for long-haul connectivity and the introduction of a middleware software infrastructure for mitigating data loss through back-pressure in summer 2009. On the sensor side extensions took place in 2009 with a remote controlled high-resolution visible light camera~~and a standard steerable webcam used for site surveying including remote control capability for the cameras and power supplies~~ (Keller et al., 2009b, a) as well as a significant extension of the crackmeters in summer 2010 and the installation of a high-precision survey-grade GNSS receiver at the very end of 2010~~in the context of the X-Sense project (Beutel et al., 2011) funded by nano-tera.ch~~ (Beutel et al., 2011). A local weather station was added in 2010 and a net total radiometer in 2015. After this first research phase focusing on prototyping and the investigation of surface kinematics ~~w.r.t.~~ with respect to thermal forcing (Hasler et al., 2012; Weber et al., 2017) an additional research avenue was added from 2012 onwards: ~~A~~ a first pilot study using acoustic emission and based on similar efforts undertaken at the Jungfraujoch ~~(Girard et al., 2012, 2013)~~ (Amitrano et al., 2012; Weber et al., 2012; Girard et al., 2012, 2013) aimed at characterizing damage evolution inside the solid rock walls in 2012/2013. A larger profiling experiment (Weber et al., 2018c) has been set up to investigate signals emanating from the mountain and possible damage events with different instruments ranging from 1 Hz to 100 kHz as well as additional L1-GPS measurement points starting in 2015/2016. Finally, in an effort to establish a vertical transect of thermal measurements spanning the whole mountain (two ground surface temperature measurement points exist on the summit since 2011, maintained by Agenzia Regionale Protezione Ambiente Valle d'Aosta (ARPA VDA), Italy, permafrost boreholes maintained by PERMOS, SLF/WSL, Switzerland are located on lower elevations at the Hörnlihütte and Hirli) an extension with further ground surface temperature profiles implemented at 4003 m a.s.l. in the vicinity of the Solvay Hut higher up on the ridge has been performed. Despite its remoteness and exposure this field site is actually readily accessible being situated directly on and in the bottom segment of the climbing route with further infrastructure nearby (mountain hut, heliport, transportation facilities, Internet connectivity) and therefore can be accessed even in a day trip from Zurich.

After completing the first ten years since the first experiment went live in July 2008 it's now time to publish a first digest of this data including a thorough documentation in order to (i) preserve this data and (ii) make it available for future research in the broader context. The data presented in this publication constitutes a best-of of the most relevant and descriptive geo-science related data collected. There are further data available in the context of this work, that either (i) have been published elsewhere (Weber et al., 2018a; Meyer et al., 2018), (ii) is not deemed suitable for publication in the context of this publication (either out of scope or to complex or too poor in quality) and (iii) have been collected by related activities in the vicinity of this field site. The most relevant of these additional data sources are described in brief in Section 4.8 in order to give the reader the relevant pointers in this context.

3 Instrumentation technology and data management

The core instrumentation technology employed at this field site are autonomous, low-power wireless networked sensors (Beutel et al., 2009), frequently also referred to as wireless sensor network or short *sensor network*. The promise of this novel technology at the time of the conception of this field site in 2006-2007~~(Hasler et al., 2008)~~ (Hasler et al., 2008) was to allow unobtrusive, large-scale and highly reliable measurements ~~with minimum failures and few interventions necessary together with the reduced resource footprint necessary allowed to pursue novel instrumentation concepts compared to traditional approaches using a single centralized data logger and squid cabling (Hasler et al., 2008). As such it was a goal from the onset of~~ based on a minimum resource footprint without a central point of failure and extensive cabling. Apart from geoscience investigations the first PermaSense project ~~(Hasler et al., 2008)~~ pursued the goal to develop means for long-term, high-quality sensing in harsh environments, generating better quality data, with online data access in near real-time~~resulting in~~ (Hasler et al., 2008). Using such technology it would be possible to achieve measurements that previously have not been possible and ~~as consequentially enabling~~ consequentially to enable new science, answering fundamental questions related to decision making, natural hazard early-warning. For selected sensors, where the integration as low-power wireless sensor was infeasible or impractical, industry standard components have been used although they have typically been adapted and integrated with our custom network, data and power management infrastructure based on our sensor network technology. Our experience over the past decade+ shows, that using a WSN is a promising approach with superb data availability and data integrity. The sensor nodes have been running reliable and autonomous on the order of years in an extremely challenging environment and off-season/unplanned maintenance efforts are seldom necessary.

3.1 PermaSense low-power wireless sensing system

The PermaSense wireless sensor networks consists of Shockfish TinyNodes sensor nodes running the Dozer protocol stack (Burri et al., 2007) implemented in TinyOS (Levis et al., 2005). The sensor nodes are integrated on a custom Sensor Interface Board (Beutel et al., 2009) with power management, data acquisition, storage and interface protection functionality. The analog data acquisition frontend is built using a 16-bit resolution and 8-channel Σ-Δ analog to digital converter (Analog Devices AD7708) and an external precision voltage reference. The ADC is controlled by software running on the MSP430 microcontroller of the TinyNode. The data acquisition operation for both single-ended and differential measurements is configured with a static, periodic sampling rate strictly interleaving with networking operations, in our case $120\,\mathrm{s}$. Other digital sensors, e.g. on-board system health, weather station, digital pressure and temperature sensors can be attached as well using a digital bus interface~~(SDI-12, RS232, RS485, I2C, SPI)~~. The data from the sensor nodes is transferred using the Dozer ultra low-power multihop networking protocol stack (Burri et al., 2007). Data is forwarded to a central data sink, a base station, ~~based on a data collection tree~~ connected to the Internet with a period of $30\,\mathrm{s}$~~from where the data is then forwarded to a central database~~. In cases of network congestion or loss of connectivity, e.g. due to excessive snow build up or base station failures, data is kept back on local storage on every node using a mechanism called backpressure. For this a $1\,\mathrm{GB}$ non-volatile Flash memory storage (SD-card) is integrated on every node. With a power envelope of about $150\,\mu\mathrm{A}$ these wireless sensors have been in continuous operation in the field for periods up to seven years based on a single D-size $\mathrm{LiSOCl_2}$ cell (SAFT LSH-20, $13\,\mathrm{A\,h}$), although due to maintenance and upgrading activities, in practice the typical operational time on location for a single node is shorter.

Similar to the backpressure mechanism on every sensor node, the base station also contains a local database for intermittent data storage in case connectivity to the database is lost. For reasons of power efficiency the sensor network does not support synchronization to absolute reference time (e.g. UTC) but ~~rely on a~~ relies on local 1-second granularity time keeping. The local timestamp of every data sample generated on a sensor node is propagated through the Dozer network and based on the arrival time of each packet ~~on~~ at the base station (a Linux system supporting ~~global time sync using NTP/chrony~~time synchronization to a global reference) the *generation time* of the respective data sample is calculated using the method of "elapsed time of arrival" (Keller et al., 2012a). Since the forwarding network uses a dynamically changing topology it can happen that data is received out of order ~~w.r.t.~~ with respect to timing at the base station. Because of inevitable drifting behavior of all local clock sources and due to intermittent losses of end-to-end connectivity between nodes of the sensor network as well as on the TCP/IP networking segment slight jumps in the timing can occur ~~but w.r.t.~~ (a detailed analysis of the network performance is available in Keller et al., 2011, 2012b). Nevertheless, these effects are not of concern with respect to the long-term nature of the processes observed (diurnal to seasonal behavior)~~these effects are not of concern (a detailed analysis of the network performance is available in Keller et al., 2011, 2012b)~~. For the user of this data it only matters that ~~if accessing the raw streaming data~~ on accessing the online data streams on the online data portal in real-time, different timing information exists for every data sample referring to the estimated *generation time*, the time of arrival ~~on~~ at the base station and the time of storage in the data base respectively and that ~~in the immediate past significant transmission delays~~

~~can occur~~very recent data may still be incomplete (out-of-order arrival with respect to time). Once data has been downloaded, quality checked and possibly also downsampled using the tools discussed in Section 3.4 and supplied alongside with the data in this paper, possible timing artifacts are no longer of concern.

3.2 ~~Sensor integration for the low-power~~ Low data rate sensor ~~network~~integration

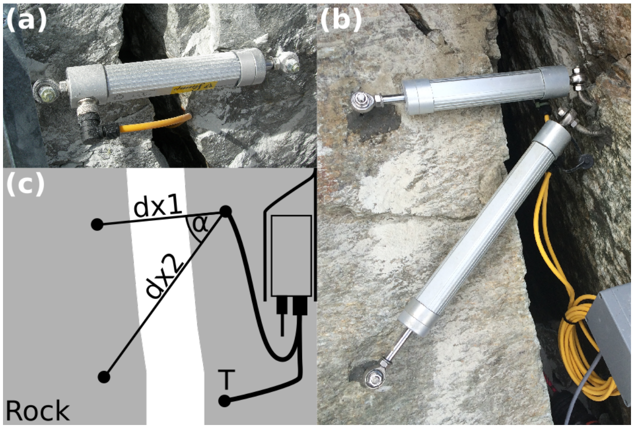

Figure 2. a) 1-axis and b) 2-axis crackmeter setup in the field. c) 2-axis crackmeter setup with one thermistor connected to the wireless sensor network. In cases where multiple crackmeters are mounted on a single location the angle α between the two crackmeters is given in combination with the length of the instrument.

The basic sensor used in combination with these wireless sensor nodes are temperature sensors (NTC thermistors) and fracture dilatation sensors (crackmeters) in different configurations ranging from single channel configurations to multiple channel configurations, e.g. 2x crackmeters and 1x thermistor (see ~~Fig.~~Figure 2b) attached to a single wireless sensor node using 3x single ended ADC channels, a half-bridge resistive divider with precision reference resistor and conversion after the Steinhart-Hart equation. A special configuration used are the rigid PermaSense sensor rod and thermistor chain (see ~~Fig.~~Figure 3). These macro-sensor assemblies incorporate multiple thermistors as well as reference resistors, an internal multiplexer circuit allowing to sense at multiple locations (depths) simultaneously housed either in a rigid glass fiber reinforced tube (sensor rod) or located inside heat-shrink tubing and cable segments configured to length as desired. Two variants exist: (i) the original $12\,\mathrm{mm}$ 4-channel sensor rod that additionally incorporates four electrode pairs allowing to measure resistivity at different depths and (ii) the revised $20\,\mathrm{mm}$ sensor rod that is designed without resistivity electrodes but rather in a configurable setup and using metal rings for better thermal coupling to the rock. Both configurations require a $1\,\mathrm{m}$ deep hole to be drilled. This most recent design is configurable ~~w.r.t.~~ with respect to the amount of sensors and the sensor depths allowing to manufacture assemblies that are compatible to commercially available units such as the UMS TH3 sensor rods that needed to be replaced as this unit is limited in its measurement range below $-20\,°\mathrm{C}$ and furthermore requires a lot of power to operate making it unsuitable for long-term monitoring.

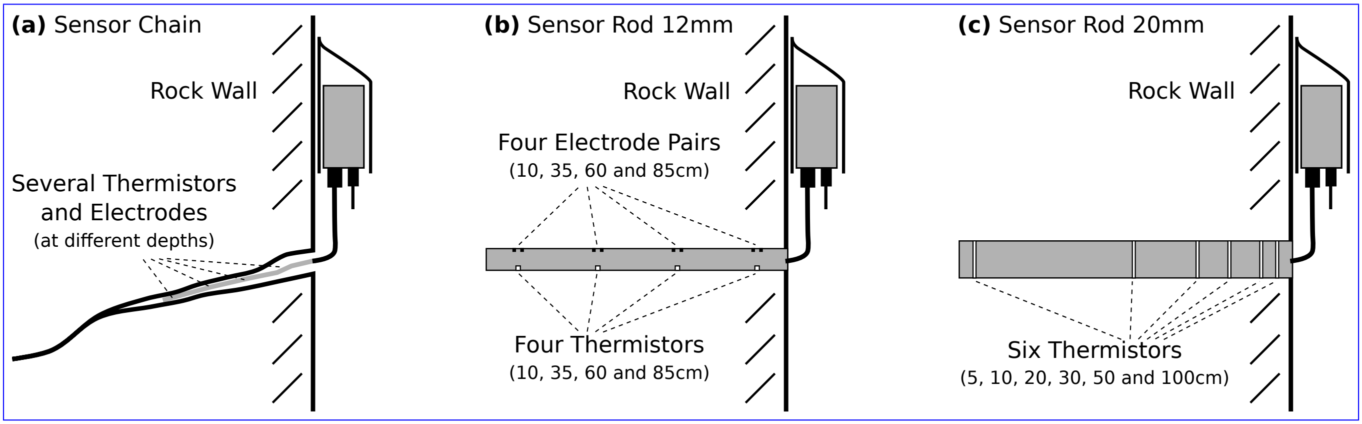

Figure 3. Sensor setup to measure temperature and resistivity in ~~fracture~~ fractures and in rock.

~~In an effort to support~~ Wireless L1-GPS ~~to be used as sensor~~ sensor nodes equipped with an additional 2-axis inclinometer for the detection of terrain movement~~in a wide-area application (Wirz et al., 2013) within such a low-power sensor network, wireless L1-GPS sensor nodes equipped with an additional 2-axis inclinometer~~ (Wirz et al., 2013) have been developed using the same principle as outlined above (Buchli et al., 2012). Only here GPS data, specifically the RAW output of the satellite observations constitutes the actual sensor data. Environmental forcing, e.g. ambient weather conditions such as air temperature, wind or radiation are measured using commercial sensors (Vaisala WXT520 weather station and Kipp & Zonen CNR4 radiometer) integrated into the sensor network.

3.3 High data rate sensor integration

A number of sensors that are not suitable for integration in a low-power and low-data rate sensor network and that typically come ready to deploy with a standard communication interface (e.g. USB, Ethernet) have been integrated into the field site as well. In order to minimize cabling ~~efforts~~ these sensing systems (e.g. ~~cameras~~a DSLR camera, high-precision GNSS reference receiver, seismic data acquisition~~systems~~) have been integrated with a Wireless LAN router and facilities to monitor and control power (switch on/off both the sensing system and WLAN from remote). Using a mix of local and remote directional link-based WLAN connectivity between the Internet and the instruments on the field site is established based on a WLAN access point located at the cable car station of the Klein Matterhorn 3883 m a.s.l. about 6.5 km away where the network is attached to a local Internet service provider using fiber.

3.4 Data management ~~- structure, metadata, procedures,~~ infrastructure~~and data access~~

Care has been taken that all data collected are structured and stored in a coordinated fashion allowing reproducible research results and re-use of data in different contexts and in future projects. Also flexibility with respect to extensions (new sensor types), support of different data rates, metadata integration and life-cycle management were taken into account. The data

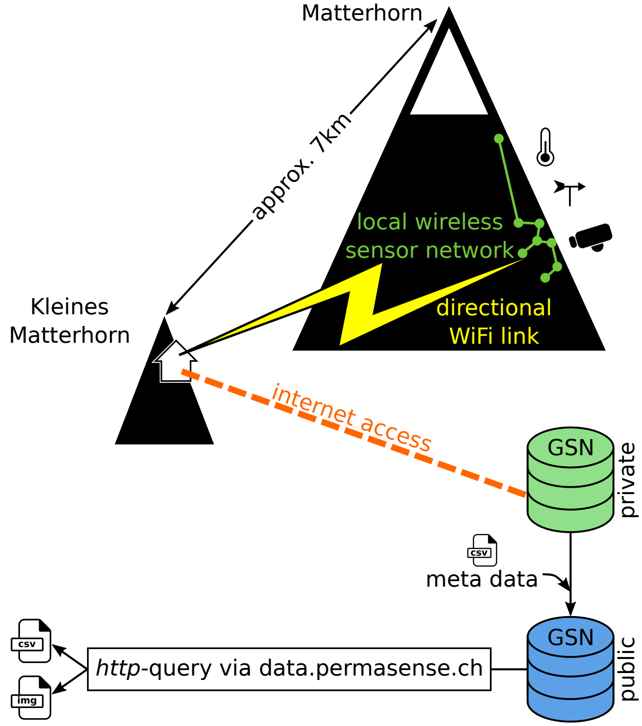

Figure 4. System architecture: ~~Data~~ data are collected with a local wireless sensor network and transmitted to the summit station of Kleines Matterhorn. The private GSN server receives the data, which are stored in a primary database. Data are passed on to a public GSN server where they are mapped to metadata (positions, sensor types, calibration, etc.) and converted to convenient data formats. Finally, data are available for download and analysis using external tools.

backend is implemented using a data streaming middleware where a dedicated processing structure called a virtual sensor is responsible for processing a specific data type, e.g. one virtual sensor for temperature measurements and another virtual sensor for images. Complete processing chains, can be implemented by concatenating virtual sensors either within the same instance of the Global Sensor Network (GSN Aberer et al., 2006) or also across multiple instances of GSN. In our case, data is processed and stored in two concatenated instances of GSN: ~~A~~ a private instance only accessible internally for primary, unprocessed data (green database instance in ~~Fig.~~Figure 4) and a public instance for secondary, processed data and publishing this data via web frontend to the user domain, i.e. the Internet (blue database instance in ~~Fig.~~Figure 4). A visualization tool provides up-to-date key graphics~~on this web frontend (Keller et al., 2012a) (see Fig.~~ (Keller et al., 2012a) on a web frontend where all all data can be accessed online at http://data.permasense.ch. Online data can be accessed using an Internet browser (see Figure **??**) or using web queries (see Appendix **??**).

~~The online data management web frontend at allows to access all data in real-time. Data are accessed by data type in entities called virtual sensors (right). Selected standard views, e.g. key graphs can be accessed via the tabs at the top.~~

In this system all data of one specific data type and processing stage is kept in a single data structure with the virtual sensor acting as its interface, i.e. all data of a specific type is kept in this respective data structure irrespective of time and location~~ete~~. The processing ~~contains~~ chains contain steps for the mapping of device IDs, sensor type and sensor IDs to positions for the respective time periods, applying the correct unit conversion functions according to the sensor type defined, decomposition of more complex data types (multiplexed data) into user-friendly data types and ~~the~~ aggregation of data~~should that be required~~. Each instance of a virtual sensor is mapped to a unique data structure, ~~and in most cases references~~ e.g. a dedicated table on a MySQL database server~~as storage resource~~. Data types with very large amounts of (binary) data, e.g. images are stored directly on a networked file system and only a reference to the respective file is stored in the database. With this two-step data management pipeline consisting of a raw data ingress, dump and store in the first instance as well as multiple processing steps as outlined in the second instance it is assured that all data transactions are consistent, transparent, traceable and verifiable. Should corrections to the data be necessary, e.g. by inclusion of further metadata, correction of metadata or the integration of alternate processing methods they can be applied by simply re-running the respective data from the private primary repository to the second instance with the modifications in place. ~~Data types with very large amounts of (binary) data, e.g. images are stored directly on a networked file system with only a reference to this file contained in the database and the GSN virtual sensor. Online access to all data is available through where all data can be accessed either via a user interface (see Fig. ??) or using standard web queries (see Appendix ??).~~

In order to consistently manage ~~this data~~ data of the field site a set of rules has been defined~~. Although this paper only discusses a single deployment or field site, the structures and procedures are actually designed to allow to manage multiple deployments from the same data management system:~~ :

- An individual protocol sheet is used for each ~~field day where interventions and other~~ intervention (field work day) where all noteworthy items are recorded (installation, maintenance, removal)
- Sensor interventions on site take place at different times for each position. To simplify things, the whole day of an intervention is typically assumed as "invalid data".
- All sensor devices are mapped to a distinct position ID. The mapping contains to-from information, the device id (possibly MAC address)~~and sensor type~~ , sensor type and calibration data.
- All data from a specific data source (sensor type) is kept in an individual data structure. Queries are typically made per data type and position ~~id~~ID.
- ~~Records about detailed~~ Detailed circumstances (crackmeter angles, thermistor depth) are ~~described in other~~ recorded using auxiliary data formats: ~~Text~~ text files, excel files or photographs.
- ~~Instance specific calibration data can be mapped using sensor type and ID.~~

As described earlier the data ingress from the base station on the field site is based on a local database on the base station that allows to delay data transmission in cases of loss of connectivity or server outages. In the first years of the deployment this functionality did not yet exist and therefore a (then significant) data gap from June to August 2009 is visible in some of the thermal and crackmeter data due to a failure in the cooling system of the server room and a longer outage of the server system. With hindsight it must be said that this outage event, that had nothing to do with the actual field site instrumentation, exemplified in an extraordinary way the need for tight integration and synchronization of storage resources at all levels of a networked sensing system.

4 ~~Field~~ Detailed field site setup and description of the primary data products

This section gives an overview as well as details of the main sensor setup installed at Matterhorn Hörnligrat and describes the data provided with this paper. Table **??** provides an overview listing of the main sensors used grouped by sensor type including their approximate period of operation, units derived, measurement interval and key sensor characteristics. ~~Figure 5 and~~ Table 2 and Figure 5 give a detailed listing of the location specific instrumentation detailing the number of sensing channels and sensor types available at each position. For every sensor type used, a detailed discussion of the specifics of each sensor type as well as installation and location specific information is given in ~~this section constituting the main detail documentation of the raw primary data presented in this paper. The respective raw primary data as described here is provided in the accompanying repositories from the beginning of each measurement until the end of the calendar year 2018. In Section 5 a number of derived data products that are additionally provided with this paper are discussed. These are downsampled and cleaned time series of the weather station, ground temperature, resistivity, fracture displacement and inclinometer data as well as GNSS daily positions.~~

~~As described in Section **??** and also visible in~~ the remainder of this section. Finally, Figure 6 ~~the sensor setup at this field site has continuously grown over the years. There are only few data gaps. The data yield and availability of the measurement systems has surpassed expectations. In a few cases (Position 2 – rockfall, Position 12 – sensor malfunctioning from initial installation) sensing positions have been retired but in general agreement exists that the sensor locations are well planned and selected and that the measurements obtained are representative for each respective location. Therefore all but the two positions mentioned have been continued to this date w.r.t. the measurement positions presented and discussed~~ gives a graphical overview of the data availability for all data products contained in this paper. ~~For the sake of completeness it must be said that a few other sensor placements exist(ed) but due to their experimental nature and/or instability they are not part of this publication.~~

~~Overview of the field instrumentation at the Matterhorn Hörnligrat: a)+b) South and North side on approximately 3500 m a.s.l. next to the 2003 rock fall event. c) Extension next to the Solvay Hut on 4003 m a.s.l. with South exposition.~~ As described in Section 2 and also visible in Figure 6, the sensor setup at this field site has continuously grown over the years. There are only few data gaps. The data yield and reliability of the measurement systems has surpassed expectations. In a few cases (Position 2 – rockfall, Position 12 – sensor malfunctioning from initial installation) sensing positions have been retired but in general agreement exists that the sensor locations are well planned and selected and that the measurements obtained are representative for each respective location. For the sake of completeness it must be said that a few other sensor placements exist(ed) but due to their experimental nature and/or instability they are not part of this publication.

Table 1. Instrumentation by position and sensor types.

	Rock					Fracture			
Position	Temperature near-surface	Temperature 5 – 100 cm	Resistivity 5 – 100 cm	GNSS observables, coordinates	Inclination	Temperature near-surface	Temperature 5 – 300 cm	Resistivity 10 – 300 cm	Displacement
MH01	2								1
MH02	1						3		1|2[b]
MH03	2						7		1
MH04							5		1
MH05							4	4	
MH06	2								2
MH07							4	4	
MH08									2
MH09						1			3
MH10	1	4	10						
MH11	1	4|6[a]	10|0[a]						
MH12	1	4	10						
MH15				in situ radiometer					
MH18									1
MH19				time lapse photography					
MH20									2
MH21									2
MH22									2|1[c]
MH25				in situ weather station[d]					
MH27		6|6[a]							
MH30		6							
MH33				1	1				
MH34				1	1				
MH35				1	1				
MH40				1					
MH42 / HOGR				1					
MH43				1					
MH46		6							
MH47		6							

[a] Intervention: change of sensor type. [b] Intervention: replacement and extension from 1-axis to 2-axes setup. [c] Intervention: one crackmeter broke due to rock fall. [d] Continuous sampling mode: 2016-12-01 – 2017-07-27 (but not 2017-06-28 – 2017-07-01), device change on 2018-09-15

Table 2. Instrumentation by position and sensor types.

	Rock					Fracture			
Position	Temperature near-surface	Temperature 5 – 100 cm	Resistivity 5 – 100 cm	GNSS observables, coordinates	Inclination	Temperature near-surface	Temperature 5 – 300 cm	Resistivity 10 – 300 cm	Displacement
MH01	2								1
MH02	1						3		1|2[b]
MH03	2						7		1
MH04							5		1
MH05							4	4	
MH06	2								2
MH07							4	4	
MH08									2
MH09						1			3
MH10	1	4	10						
MH11	1	4|6[a]	10|0[a]						
MH12	1	4	10						
MH15				in situ radiometer					
MH18									1
MH19				time lapse photography					
MH20									2
MH21									2
MH22									2|1[c]
MH25				in situ weather station[d]					
MH27		6|6[a]							
MH30		6							
MH33				1	1				
MH34				1	1				
MH35				1	1				
MH40				1					
MH42 / HOGR				1					
MH43				1					
MH46		6							
MH47		6							

[a] Intervention: change of sensor type. [b] Intervention: replacement and extension from 1-axis to 2-axes setup. [c] Intervention: one crackmeter broke due to rock fall. [d] Continuous sampling mode: 2016-12-01 – 2017-07-27 (but not 2017-06-28 – 2017-07-01), device change on 2018-09-15

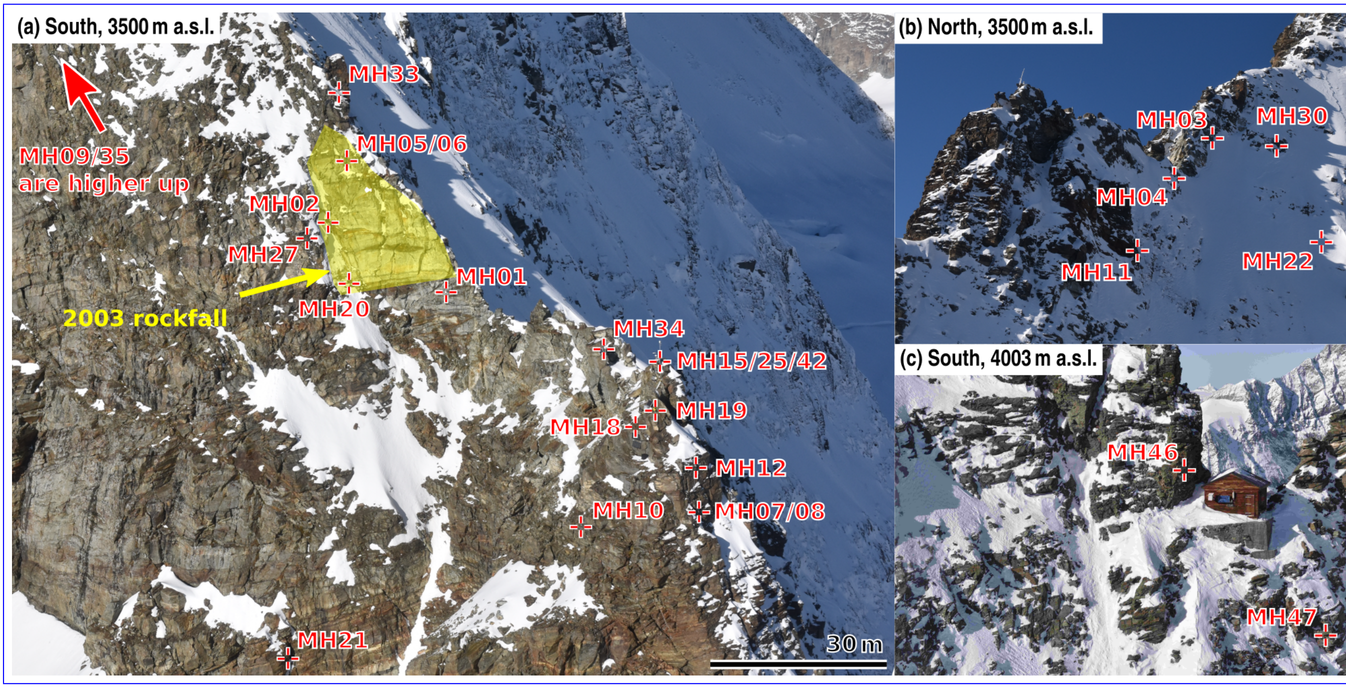

Figure 5. Overview of the field instrumentation at the Matterhorn Hörnligrat: a)+b) South and North side on approximately 3500 m a.s.l. next to the 2003 rock fall event. c) Extension next to the Solvay Hut on 4003 m a.s.l. with South exposition.

4.1 Weather station data

~~Meteorological data have been recorded both in Switzerland as well as in Italy over many decades. The closest comprehensive meteorological data record relative to the Matterhorn field site are the MeteoSwiss stations Stafel (VSSTA), Findelen (VSFIN), Gornergrat (GOR), Monte Rosa Plattje (MRP) and Zermatt (ZER), the MeteoGroup station Kleines Matterhorn as well as the stations of the Intercantonal Measurement and Information System (IMIS) ZER1, ZER2, ZER4 and GOR2. If required, these data have to be retrieved from the respective data owners.~~

Since 2010 a local weather station based on a Vaisala WXT520 compact all-in-one weather instrument is installed on-site to obtain a more detailed weather data record comprising ambient air temperature (see black line in Figure 7), air pressure, relative humidity, wind (speed and direction) and precipitation. This has been extended with a 4-component net radiometer Kipp & Zonen CNR4 in the summer of ~~2015.~~ 2015 (see green line in Figure 7 for shortwave radiation in). The net radiometer is installed without capabilities for ventilation and heating. The WXT520 is capable of heating the rain and wind sensor but for practical reasons this feature is only enabled when enough power is available which typically corresponds to good weather periods and turned off especially in prolonged bad-weather periods. Both instruments have been vendor calibrated and the respective calibration data is applied in the data conversion procedures as advised by the manufacturer. It is well known that it is not straightforward to measure present weather conditions in such a hostile and exposed location, high up on the ridge of a

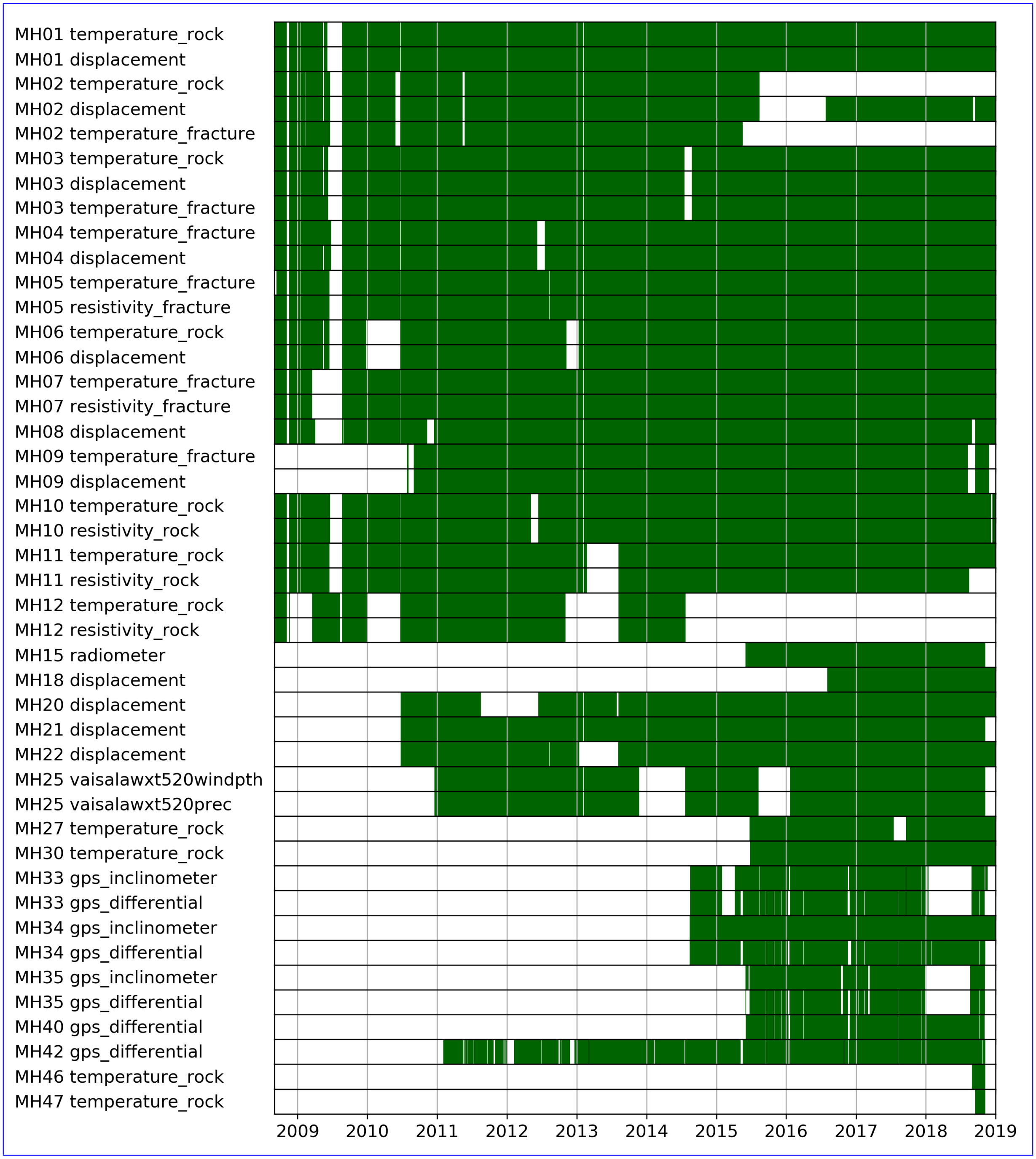

Figure 6. Data availability for all data products. The time periods when data is available are indicated in green.

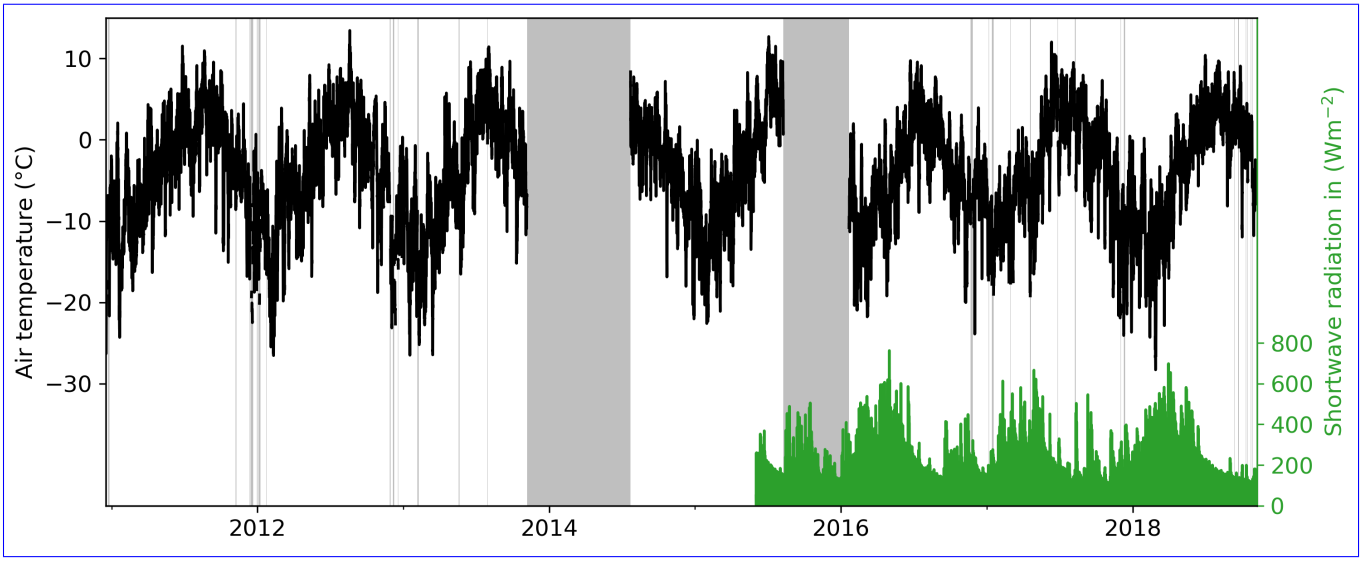

Figure 7. Air temperature and shortwave radiation data. Gray bars indicate data gaps.

4000 m peak. Therefore this data must be treated with some caution. There are more data outages as with our other sensors. Clearly an instrument such as the Vaisala WXT520 designed to measure liquid precipitation (with the principle of counting and integrating over the impacts of droplets on the sensor surface) is neither designed nor capable of measuring solid precipitation in any form. Further, the Vaisala WXT520 has been operated in different modes (interval vs continuous sampling) which resulted in different maximum/minimum wind velocity data. Also the application of a net radiometer on a high-alpine rock ridge is far from any WMO compliant sensor setup. Although in parts only indicative, the data obtained from these sensors is very valuable as it is local to the site and exhibits all the small scale local and temporal variability that regional models extrapolating from national service weather data cannot capture, e.g. regular local cloud build up on the mountain slopes in the summer's late afternoons, detailed onset timing of local weather changes etc.

4.2 Ground temperature

Ground temperature data ~~describes temperature measured~~ are recorded at different depths (ranging from ~~near surface~~ near-surface, which refers to a depth of $3-8\,\mathrm{cm}$, to $3\,\mathrm{m}$ depth) inside fractures as well as in intact/solid rock. All measurement devices use NTC (Negative Temperature Coefficient) thermistors potted in epoxy and ~~were~~ calibrated with zero point calibration at ~~0° C~~ $0\,°\mathrm{C}$. Beside the single thermistor setup to measure near-surface temperature, two different major types are used to measure temperature at different depth: ~~On~~ on the one hand sensor rods are drilled in the rock and on the other hand thermistor chains are deployed in fractures (see Table **??**). All thermistor systems used have been calibrated using a single-point calibration scheme at $0\,°\mathrm{C}$. The main characteristics of the four different temperature measurement devices used are given in the following~~.~~ ~~All thermistor systems used have been calibrated using a single-point calibration scheme at 0 °C~~:

1. PermaSense sensor rod 12 mm:
   YSI-44006 NTC thermistors, interchangeable tolerance ±0.2 °C, Drift @ 0 °C over 100 months <0.01 °C
2. UMS TH3 sensor rod 20 mm:
   Digital system with built in ~~ADC~~analog to digital converter (ADC). ±0.1 °C, measuring range −20 °C to 50 °C, resolution. 0.034 °C
3. PermaSense sensor rod 20 mm:
   Measurement Specialities epoxy encapsulated 44031RC NTC thermistor mounted inside aluminum contact rings with thermally conductive epoxy, interchangeable tolerance ±0.1 °C , Drift @ 0 °C over 100 months <0.01 °C
4. Various thermistor configurations (single or embedded in sensor chain):
   YSI-44006 NTC thermistors, interchangeable tolerance ±0.2 °C, Drift @ 0 °C over 100 months <0.01 °C

Table 2 shows which temperature sensors are installed at which position, whereas Table 3 the depths of the thermistors. Figure 8 shows exemplary hourly rock temperatures measured at 10 cm and 85 cm depth and mean annual rock temperature at 85 cm (MAGT_85cm) for years with more than 98% data availability.

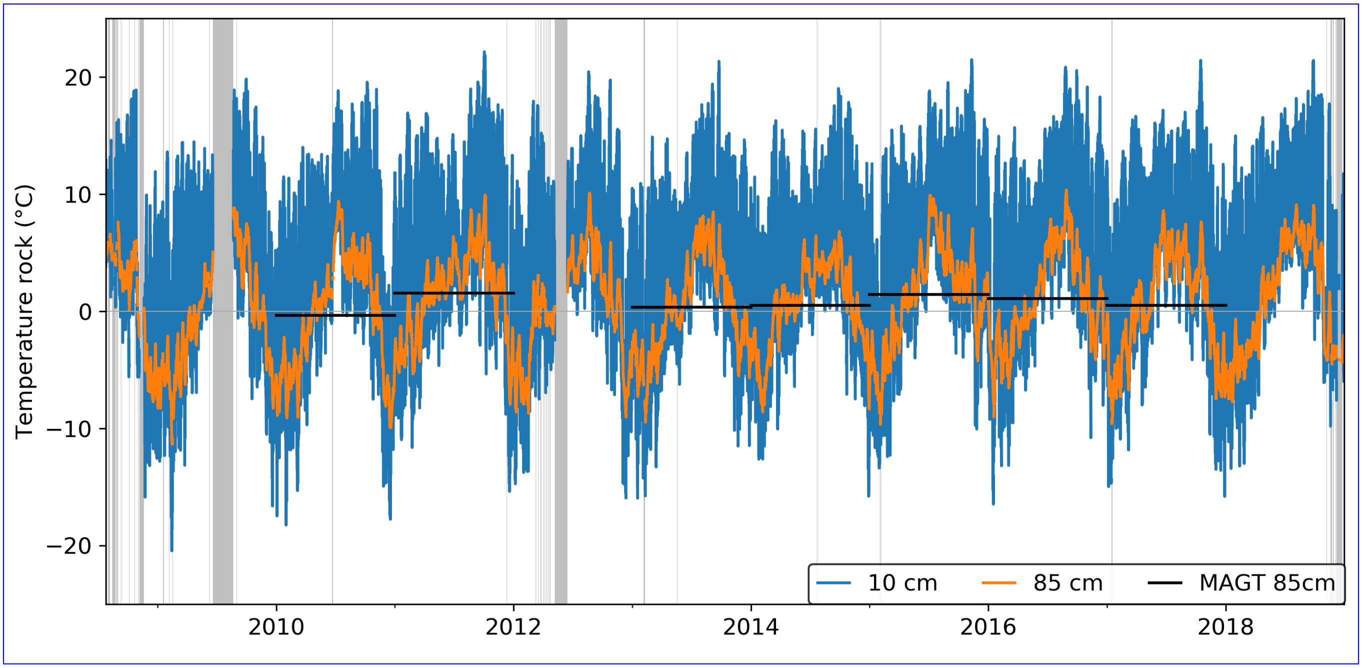

Figure 8. Rock temperature measured at different depths at position MH10. Black lines indicate mean annual rock temperature at 85 cm depth~~(MAGT 85 cm~~, if at least 98% of the data are available. Gray bars indicate data gaps.

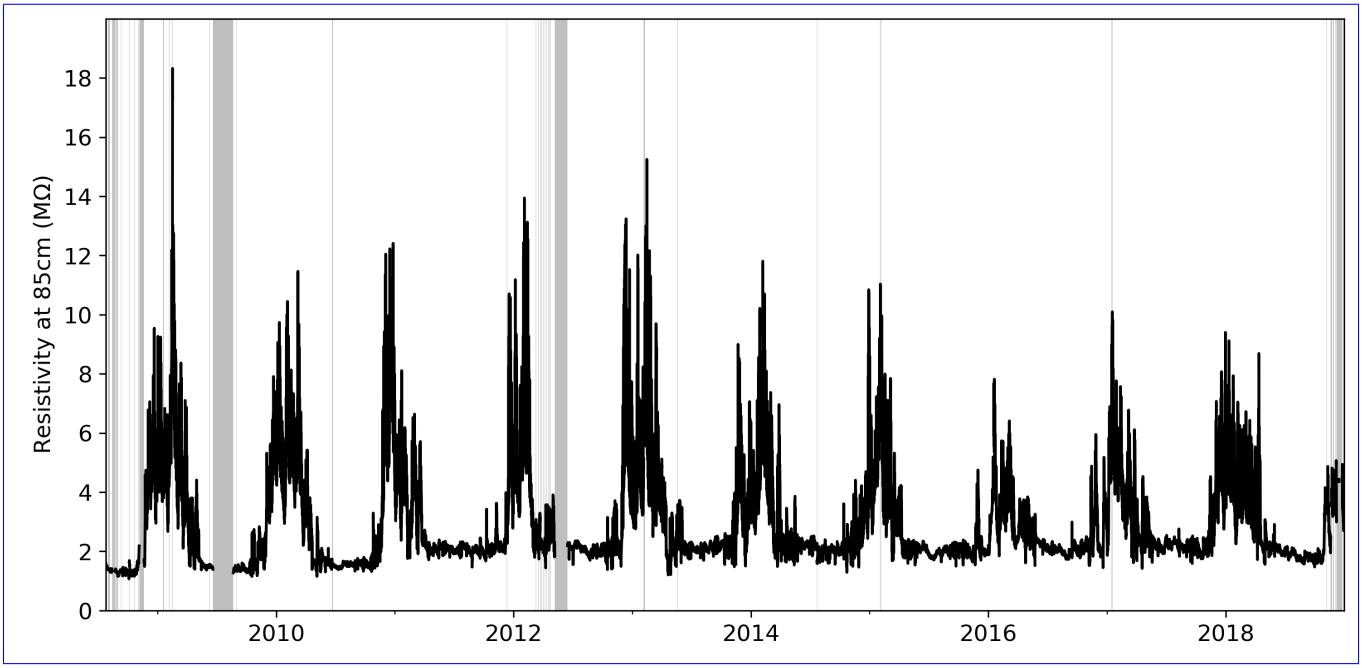

Figure 9. Resistivity time series measured at 85 cm depth in an intact rock wall at position MH10. Gray bars indicate data gaps.

4.3 Ground resistivity

Electrical resistivity tomography (ERT) is a common geophysical method to characterize ~~sites w.r.t. high-resolution insight into~~ the shallow subsurface (Daily et al., 2012). ERT has successfully been used to observe temporal and spatial variations of moisture movement during freeze-thaw cycles in solid rock faces (Sass, 2004, 2005) and in solid permafrost rock walls in short- (Krautblatter and Hauck, 2007) and long-term (Keuschnig et al., 2017) measurement campaigns.

The PermaSense sensor rod 12 mm is designed with four electrode pairs with a distance of a centimeter each that couple with the rock electrically using conductive foam pads (see ~~Fig.~~Figure 3). In contrast to ERT-surveys, here the contact resistance is directly added to the rock resistance (serial connection). The direct current (DC) flowing through of the rock is measured when excited with a reference voltage (i) at these electrode pairs (at the same depth) in order to gain an indication into the liquid water content and (ii) between electrodes at different depth using and sensor-internal multiplexing unit. The latter configuration has to be interpreted carefully due to the extremely high resistances of this configuration (resistance measurements depend on the contact resistance of the electrodes and on local heterogeneity of the rock between these electrodes). While Table 3 provides the depths of the electrodes for each position, Figure 9 indicates a strong seasonal pattern, which is most likely related to the freezing of the rock. Comparable to the results of a study by Krautblatter (2009), temperature-resistivity gradients for intact porous rock in frozen state here lie in a similar range of about $20 - 40\%/^{\circ}\mathrm{C}$ cooling (Hasler, 2011).

Table 3. Depths of thermistors and electrodes by position and medium under investigation.

Position	Medium	Depths (cm) of thermistors[a]	Depths (cm) of electrodes
MH02	Fracture	10, 30, 70	none
MH03	Fracture	10, 40, 60, 70, 75, 80, 85	none
MH04	Fracture	5, 20, 30, 35, 40	none
MH05	Fracture	10, 80, 150, 180	10, 80, 150, 180
MH07	Fracture	10, 100, 200, 300	10, 100, 200, 300
MH10	Rock	10, 35, 60, 85	9.5, 10.5, 34.5, 35.5, , 59.5, 60.5, 84.5, 85.5
MH11	Rock	10, 35, 60, 85 |[b] 5, 10, 20, 30, 50, 100	9.5, 10.5, 34.5, 35.5, , 59.5, 60.5, 84.5, 85.5 |[b] none
MH12	Rock	10, 35, 60, 85	9.5, 10.5, 34.5, 35.5, , 59.5, 60.5, 84.5, 85.5
MH27	Rock	5, 10, 20, 30, 50, 100	none
MH30	Rock	5, 10, 20, 30, 50, 100	none
MH47	Rock	5, 10, 20, 30, 50, 100	none
MH46	Rock	5, 10, 20, 30, 50, 100	none

[a] Excluding single near-surface thermistors. [b] Intervention: change of sensor type.

4.4 Fracture displacements

Fracture displacements are measured using Stump/Terradata ForaPot crackmeters. These instruments are very accurate and robust linear potentiometers that are digitized using the wireless sensor ~~networks~~ nodes described earlier using a resistive half-bridge connection and a single-ended ADC channel per sensor element similar to the temperature measurements. The sensors exhibit a high linearity of $\pm 0.075\,\%$ (50-150mm measurement range) and $\pm 0.05\,\%$ (200-300mm measurement range) with a resolution better than $0.01\,\mathrm{mm}$ and a temperature dependant drift of max. $5\,\mathrm{ppm}/^{\circ}\mathrm{C}$ i.e. $0.25\,\mathrm{\mu m}/^{\circ}\mathrm{C}$ for a change of $10\,^{\circ}\mathrm{C}$ on a $50\,\mathrm{mm}$ range instrument. The devices are specified for operation in -30 to $100\,^{\circ}\mathrm{C}$. The setup has been validated on site ~~w.r.t.~~ with respect to device interchangeability and long-term stability, the details of which can be found in (Hasler et al., 2012) and the appendix of A. Hasler's PhD thesis (Hasler, 2011).

Table 4. Metadata describing all crackmeter sensors measuring fracture displacements, extended after (Weber et al., 2017).

Position	1st Crackmeter	2nd Crackmeter	3rd Crackmeter	Aspect	Slope	Fracture Characteristics
MH01	50 mm[a]	-	-	95° N	75°	intense solar radiation, microcracks next to main south facing fracture
MH02[b]	50 mm	150 mm[c]/−45°	-	80° N	50°	wet fracture system in main detachment zone, concave, often snowy
MH03	150 mm	-	-	350° N	65°	north-oriented, lower part ends in snow flank
MH04	50 mm	-	-	320° N	70°	debris ledge north of small saddle
MH06	100 mm	200 mm/−90°	-	90° N	60°	south facing corner on ridge, often snowy
MH08	100 mm	150 mm	-	50° N	90°/47°	wide, ventilated, shadowed main fracture
MH09	100 mm	200 mm/54°	200 mm/7°	120° N	65°	leaning tower buttress on top couloir exit
MH18	150 mm	-	-	140° N	20°	flat fracture, winter snow accumulation
MH20	150 mm	150 mm/−60°	-	70° N	70°	bottom part of the fracture system in the main detachment zone , often snowy, wet fracture
MH21	100 mm	200 mm[d]/−40°	-	70° N	85°	wide open, south exposed fracture on pillar below the detachment zone
MH22	100 mm	150 mm/55°	-	70° N	85°	fracture system on ledge in north flank

[a] Was removed for rock expansion test from 06/2010 to 12/2016. [b] The sensors were destroyed 2015-08-15 by rockfall. Crackmeters were re-equipped on 2016-07-28 but thermal measurements at this location was stopped. [c] Was 50 mm before 2016-07-28. [d] Was 150 mm before 2017-07-18.

The primary usage of these instruments is to determine displacements perpendicular to a fracture, i.e. the opening and closing movement (see ~~Fig.~~ Figure 2a). At select locations multiple crackmeters have been installed in order assess movement both perpendicular as well as parallel to the fracture (shearing) (see ~~Fig.~~ Figure 2b and c). In one location (position MH09) a triple crackmeter placement has been installed in order to capture three degrees of freedom of a large buttress detaching from the ridge into the East face. The buttress itself is additionally instrumented with a L1-GPS unit and integrated inclinometer (position MH35) mounted on top of the instable structure. Table 4 lists the details of all crackmeter installations: ~~Length~~

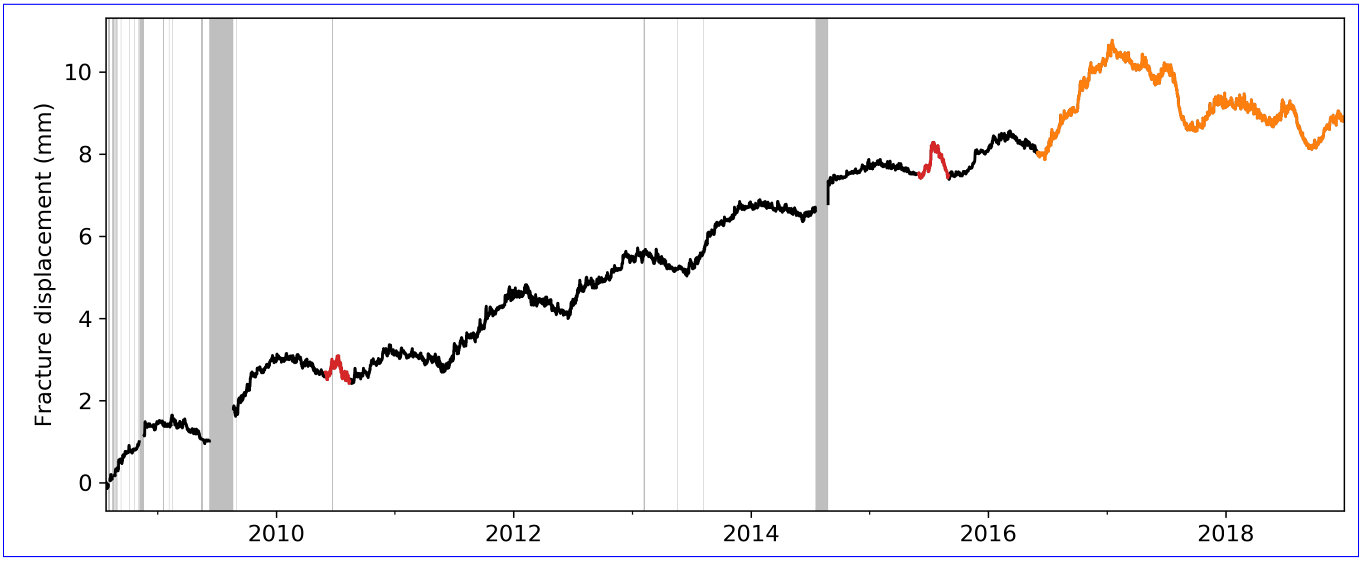

Figure 10. Fracture displacement measured perpendicular to the fracture at position MH03. Gray bars indicate data gaps.

length of each instrument, aspect, slope angle and characteristics. In cases where multiple crackmeters are mounted on a single location, the angle α between the two crackmeters (see ~~Fig.~~Figure 2b) ~~bis~~ is given in combination with the length of the instrument. Using this information it is straightforward to calculate movement vectors in other angular configurations, e.g. parallel to the fracture using trigonometric equations ~~. Examples of this method can be found here in Hasler et al. (2012) and Weber et al. (2017)~~(for details see Hasler et al., 2012; Weber et al., 2017). An example of the fracture displacement measured perpendicular to the fracture at position MH03, a north-oriented fracture in a very thin segment of the ridge that remained after the July 2003 rockfall, is shown in Figure 10. The signal shows both cyclic behavior following the annual temperature regime as well as an irreversible component continuously widening the fracture. This figure is an example that although a seemingly regular behavior can be seen for many years (see black line) it is likely that further processes are involved~~that in this caselead~~. In this case, these processes led to additional small excursions in summer 2010 and 2015 (see red lines Fig. 10) as well as to a change in the regime from ca. 2017 onwards (see orange lines Fig. 10) where the "regularity" of the preceding years is perturbed.

4.5 High-resolution visible light imaging

A time-lapse camera based on a Nikon D300 camera with a 24mm f/2.8D fixed focal length lens has been implemented using the PermaSense base station hardware and a WLAN data link (Keller et al., 2009b). The schedule and parameters for taking pictures can be remotely managed, making it possible to control the camera based on experimental needs~~remotely~~. At times when there are no imaging jobs active, the whole system sleeps minimizing overall power consumption to be woken up on request using our low-power wireless sensor network. In this manner, the camera has been operating since 2009, taking many tens of thousands of images from the field site. We have included a selection of images taken at approximately 2-hr intervals at full resolution of the camera ~~and all in JPEG format~~ (DX format sensor at 23.6 mm × 15.8 mm, 4288 × 2848 pixels, JPEG format). Further images are available in the form of a hand-selected and labeled ~~dataset~~ data set in (Meyer et al., 2018) or directly from the web frontend at http://data.permasense.ch where different resolutions and image formats are also available (select pictures in Nikon RAW (NEF) and/or in variable image resolution).

4.6 GNSS raw observation data

In order to assess large-scale movement of individual buttresses of the ridge a number of GNSS sensors are used. ~~The primary GNSS sensor is a~~ A high-performance ~~GNSS receiver~~ Leica GRX1200+ GNSS receiver with a Leica AR10 antenna ~~that~~ has been installed on the top outcrop of the lower ridge of the detachment scarp in December of ~~2010. Further low-cost~~ 2010 (position MH42/HOGR). Low-cost wireless L1-GPS systems based on a u-blox LEA ~~6-T~~ 6T receiver and a Trimble Bullet III antenna are mounted at further locations. Typically, this data is post-processed using double-differencing GPS processing along short baselines to derive daily position coordinates (see ~~Sect.~~Section 5.2). The position MH42/HOGR is acting as a reference. Since this constitutes a one-of-a-kind data set and other usages of this data are possible (Hurter et al., 2012) we are including the raw GNSS observations as well as the derived data products in this ~~dataset~~data set.

Different GNSS observables are available depending on the receiver architecture used. The raw observables are available in the form of industry standard daily RINEX 2.11 observation files for each station concerned. Position MH42/HOGR contains both GPS and GLONASS observation data for both L1 and L2 sampled at an interval of 30 s while the remaining positions are L1-GPS observations tracked at intervals of 30 s respectively 5 s (see Table 5).

Table 5. Details of GNSS observation periods and observables.

Position	Period of Operation	Observables	Sampling Interval
MH42 / HOGR	12/2010 - ongoing	C1 L1 D1 S1 P2 L2 D2 S2	30 s
MH33	08/2014 - ongoing	C1 L1	30 s
MH34	08/2014 - ongoing	C1 L1	30 s
MH35	06/2015 - ongoing	C1 L1	30 s
MH40	06/2015 - ongoing	C1 L1	5 s
MH43	08/2018 - ongoing	C1 L1	5 s

4.7 Inclinometer data

The wireless L1-GPS sensor systems installed on positions 33, 34, 35 (stations MH33, MH34, MH35, see ~~Tab.~~Table 5) also contain an integrated 2-axis inclinometer based on a MEMS component (Murata SCA830-D07). It is sampled every 120 s, support a $\pm 30\,\mathrm{mg}$ offset accuracy over the operating temperature range. The data is transmitted over the wireless sensor network and can be used to assess the rotational movement across the two horizontal axes of the rock mass as well as the height of the mast the GPS sensor is mounted on. For an example of this method see (Wirz et al., 2013, 2014) an example of the inclination change combined with displacement derived from daily GNSS position coordinates is shown in Figure 14 for position MH34.

4.8 Further data and related work

In the following, we list different data types and respective sources of data that we know exists and that is closely related to the data collated and documented in this publication and that are not available through a well established (national) data service e.g. weather service or cartographic service. It is a mixture of data that either we obtained by ourselves but is out of scope of this publication either (i) because it is specific to a campaign or purpose, (ii) not mature enough in the sense of quality control and processing or (iii) owned by a related (research) project effort. Nevertheless we take the opportunity to list the data sources we are currently aware of as of writing of this publication. For access to the respective data please contact the data owners given in the references.

4.8.1 Meteorological data

The closest comprehensive meteorological data record relative to the Matterhorn field site are the MeteoSwiss stations Stafel (VSSTA), Findelen (VSFIN), Gornergrat (GOR), Monte Rosa Plattje (MRP) and Zermatt (ZER), the MeteoGroup station Kleines Matterhorn as well as the stations of the Intercantonal Measurement and Information System (IMIS) ZER1, ZER2, ZER4 and GOR2. If required, these data have to be retrieved from the respective data owners.

4.8.2 Acoustic and microseismic data

Since 2012 a number of different experiments investigating acoustic emission (Weber et al., 2018c), microseismic signals (Weber et al., 2018b) using different instruments ranging from piezoacoustic sensors (>5 kHz), accelerometers (10 Hz-10 kHz) and seismometers (1-100 Hz) have been conducted. The respective data sets for these publications are publicly available and described in detail here (Weber et al., 2018a; Meyer et al., 2018). While the acoustic emission and mid-frequency accelerometer data is highly site specific and experimental, the lower frequency seismometer data is of a more general interest and applicability. Since the end of 2018 this data is being propagated automatically to the Swiss Seismological Service (SED) at ETH Zurich where it is curated and can be accessed online.

Further seismic data originating in a measurement campaign of ARPA VDA, Italy from 2007 to 2012 near the J.A. Carrel hut on the south-east ridge of the Matterhorn at 3829 m a.s.l. is also available (Coviello et al., 2015; Occhiena et al., 2012).

4.8.3 Aerial imaging campaigns

In the year 2013 the UAV company senseFly in collaboration with Pix4D and Drone Adventures performed a demo flight with their UAV drones covering the whole Matterhorn from summit to base. From this campaign a 300 million points 3D pointcloud as well as orthophotos exists. Complementary imaging and scanning products are available by Swisstopo (www.swisstopo.admin.ch).

4.8.4 Terrestrial laserscanning and radar campaigns

Several campaigns using terrestrial laserscanning (TLS) with instruments located both on the Matterhorn Hörnliridge and near the Hörnlihütte below (in 2014, 2015, 2016, 2018) as well as two real aperture radar interferometry (Caduff et al., 2015) campaigns (2015, 2016) have been performed. This data can be obtained from the authors upon request.

4.8.5 Permafrost thermal data

A number of permafrost monitoring boreholes exists in the vicinity. The closest relative to our site are the PERMOS borehole Matterhorn (MAT_0205) ~~(Luethi and Phillips, 2016; ?)~~ (Luethi and Phillips, 2016; PERMOS Database 2019, 2019; Noetzli et al., 2019) located at the Hörnlihütte at 3270 m a.s.l. and two shallow boreholes located at the J.A. Carrel hut on the Italian ridge (Coviello et al., 2015; Occhiena et al., 2012). Further downslope are the Cima Bianche field site managed by ARPA VDA and located on the Italian side (Pogliotti et al., 2015) at 3100 m a.s.l and another borehole managed by SLF/Zermatt Bergbahnen and located on the Swiss side at Hirli near the ski lift station at 2775 m a.s.l. Together with two GST temperature loggers located at the Matterhorn summit and operated by ARPA VDA this data constitutes a unique transect both ~~w.r.t.~~ with respect to the altitude profile but also the exposition. Up the south side, over the summit and down the northeast.

4.8.6 Wireless network related technical data

A large amount of data concerning sensor status and health, network performance, solar power generation etc. is available over the whole deployment period. The PermaSense wireless sensor network on the Matterhorn constitutes the longest running sensor network for scientific (research) purposes worldwide and arguably also in an extreme environment. This data can be accessed through our online data portal at http://data.permasense.ch but publishing this data within this publication is out of scope.

5 Derived data products, processing and validation methodology

For a select amount of the primary data provided with this paper we present ~~a number of~~ derived data products~~as well as the processing and validation methodology used in the following.~~ : A number of data sources exhibit very high sampling rates. Depending on the analysis goals these high sampling rates (e.g. 120 s) can be seen as an asset, e.g. to understand small scale, short term process chains but in general when dealing with the whole ~~dataset~~ data set over a decade the gigantic amount of these data constitutes a burden. Therefore, we first introduce a method to downsample these data to reasonable rates in combination with a few data cleaning steps that have emerged as successful out of good practice. ~~We provide both a description of the method, the code implementation as well as all input and output data in the context of this paper. Therefore the reader can adjust the proposed data processing steps at will using our template code should that be required. Specifically~~Specifically, this method includes (optional) filtering based on sensor-integrated reference resistors (for thermistors and crackmeters), data cleaning based on the manual interventions recorded and the temporal aggregation over 1-hour windows. The resulting data products are file sizes in the order of 100 kB per year rather than 100's of MBs. We provide both a description of the method, the code implementation as well as all input and output data in the context of this paper to allow full transparency and reproducibility. Furthermore by providing a toolset used for all processing steps concerned the reader can adapt processing steps or update the data set independently from future data set updates (living data process).

~~The GNSS raw data is processed~~ In the case of the GNSS data the raw GNSS observables are processed to daily positions using double-differential ~~GPS~~ post processing and a local geodetic network ~~yielding daily position coordinates as resulting data products (see Sect. 5.2for details)~~as described in Section 5.2. A description of the processing toolset is available in Appendix **??**.

5.1 Weather station, ground temperature, resistivity, fracture displacement and inclinometer derived data products

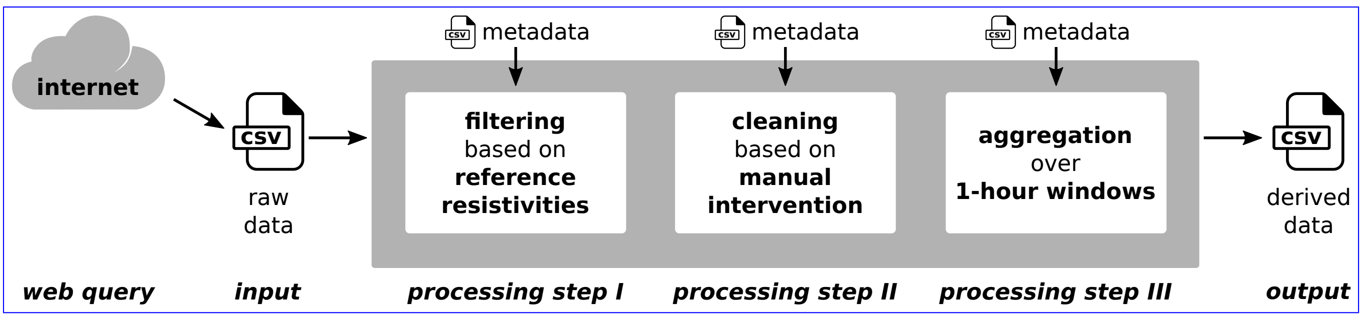

Figure 11. Three-step data processing methodology for PermaSense sensor data.

The data stored in the PermaSense GSN public database contains data obtained from sensor nodes after unit conversion. These data that, we call *raw data* can be downloaded using a standard web query (see Appendix **??**). However, since these data are sampled and transmitted independently they do not have a common time stamp and can at times contain discrepancies such as spurious outliers or the response to anthropogenic interventions, e.g. on manual service days. Therefore, a multi-step data processing methodology (see ~~Fig.~~Figure 11) is applied, where each step is optional/user selectable (details are given in Appendix **??**):

Step I: ~~Filtering~~ filtering based on reference resistivity data[1] Independent additional electrical resistors are built into the PermaSense sensor chain, PermaSense sensor rod 12 mm and PermaSense sensor rod 20 mm as a means to assess sensor and data integrity (detailed description is given in ~~Sect.~~Section 4.2 and 4.3). After filtering using these reference values, only data with reference resistivity values within a given range (defined in the metadata) are considered for further propagation.

Step II: ~~Cleaning~~ cleaning using a lookup-table Artifacts in the data either identified manually or systematically known (e.g. on device change interventions) are cleaned using this step. Cleaning operations are *delete*, *set an offset* or *replace* a single or multiple data points.

Step III: ~~Aggregation~~ aggregation over 1-hour windows For all data types but GNSS data and photographs 1-hour aggregates are calculated. For most data types, the aggregation function *arithmetic mean* was applied. Different aggregation functions were applied to some meteorological data, as an example *sum* for rain duration or *maximum* for rain peak intensity. For details, see Table **??** in Appendix **??**.

5.2 GNSS derived data products

~~Differential GPS processing workflow.~~

Daily static positions for all GNSS stations are calculated using double-differential GPS post processing based on two different tool chains: ~~Using~~ using the Bernese GNSS Software (Dach et al., 2015) and the open-source RTKLIB toolchain (Tomoji, 2018). For processing the observables are first collected from the online database and stored in daily observation files with one file per day and position. Double-differencing achieves best accuracy when utilizing the precision final GNSS data products from IGS although other GNSS data products can be used as well. In a final step the position coordinates are converted from WGS84 coordinates to Swiss national coordinates using the online REFRAME conversion service (REST API) by swisstopo. The resulting position data is subsequently uploaded again to the GSN database server from where it can be queried. The geodetic datum of all daily position data is CH1903+/LV95 with the reference frame Bessel (ellipsoidal). After post-processing data for a required amount of days, position data for each position is collated in a single file per position and a number of standardized graphs are generated (see ~~Fig.~~ Figure 12).

Apart from the raw GNSS observations in the form of daily RINEX 2.11 files we provide the calculated daily positions for both processing toolchains as described above. Further, we provide the scrips and configuration files used to run the open-source RTKLIB toolchain both from prepared RINEX files and from the online data from our database (see Appendix **??**). Double-differential GNSS processing (Teunissen and Montenbruck, 2017) is based on data obtained in a common observation interval from a station pair. Positions for the so-called "rover" can be calculated with high accuracy under the assumption that the "reference" station location is quasi-stationary and that observations from both stations are subject to similar perturbations. In practical application of this technique care should be taken that the baseline distance between any station pair is short, the field of view to the satellites (horizon) is similar and that a station pair be located in the same altitude regime. Main quality indicators of the input data (GNSS observables) are the number of visible satellites, the signal-to-noise ratio and the observation duration. For the derived data products the ratio of fixed ambiguities as well as the standard deviations per coordinate axis are the key indicators.

~~In the case of the GNSS positions at Matterhorn Hörnligrat all rover positions MH33-MH40, MH43 (the L1-GPS systems) are calculated relative to the two-frequency high-performance GNSS receiver located at MH42/HOGR. However this reference location is also exhibiting significant movement as it is positioned on the top of the buttress between the detachment zone in~~

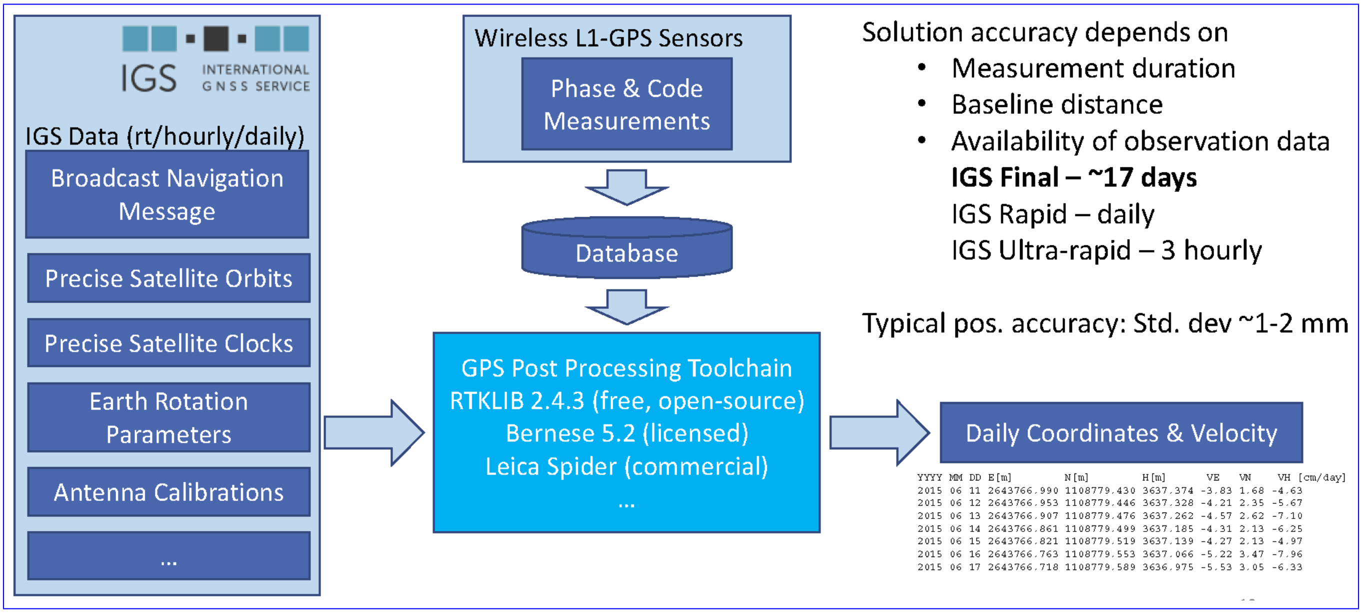

Figure 12. ~~Relative displacement of the GNSS positions measured at Matterhorn Hörnligrat. For an approximate overview of the measurement setting see Figures ?? and ??~~Differential GPS processing workflow.

~~the second couloir and the first couloir. Therefore the absolute position output of positions MH33-MH40, MH43 contains the movement of the reference position MH42/HOGR. In order to quantify this movement and remove the differences from the rover positions MH33-MH40, MH43 precise absolute positions for MH42/HOGR are calculated using a longer baseline to the non-moving reference station of the Automated GNSS Network of Switzerland (AGNES) operated by swisstopo with station ZERM located at Furi, Zermatt, Switzerland, 1867 m a.s.l. The daily position data series provided with this paper contain the uncorrected position data. Calculating the corrected position values by differencing is straightforward. An example of such corrected data (the relative displacement of the positions MH33-35 and MH42/HOGR) can be seen in Figure 15. Similarly calculating velocities or aggregate displacements using a simple or more complex method (Wirz et al., 2014) is at the discretion of the data user.~~

5.3 Cross-validation of different sensor data: Examples

~~Displacement (MH08, dx2), resistivity (MH10, 85cm) and relative 3D coordinates derived from L1/L2 GNSS (MH42/HOGR) plotted against rock temperature (85cm) at position MH10.~~

In this section we are giving a few select examples of data originating from different sensors plotted side-by-side in order to put this data into context. The few examples shown can by no means be exhaustive and are meant only as indicative examples to showcase some selected data in a visual format. We are only giving a brief introduction and interpretation in the following.

Detailed analysis using further methods, especially by leveraging correlation methods that allow to combine data from different sensor types, should be applied to this data, but this is clearly beyond the scope of this paper.

In Figure 13 we showcase three types of data in a format suitable for the analysis of frozen ground: Fracture displacement measured using a crackmeter, rock internal resistivity and relative displacement measured using GNSS side-by-side and plotted against temperature, the different years are color coded in order to understand the behavior over time. The data shown originates from four different sensor types at three different locations. All three plots show freeze-thaw related processes that repeat each year as well as an irreversible kinematic component that dominates in summer when temperatures in the rock wall are well above zero.

Similarly, stepwise displacements can be seen when plotting GNSS derived daily positions and a co-located inclinometer on a conventional plot using time on the X-axis (see ~~Fig.~~Figure 14). The first thing to note in this plot is the fact that different sensors and their resulting data types exhibit significantly different error patterns. Here, although the displacement is only on the order of millimeters, the GNSS derived displacements are much more accurate/stable than the inclinometer data that seem to be heavily influenced by present weather conditions, e.g. wind. Over winter periods, the displacement is negligible while the inclinometer raw data apparently relaxes. With the onset of the snow-melt period, an acceleration takes place that can be seen both in the GNSS data as well as the inclinometer. This acceleration continues until late fall. The exact timing of this behavior is known from in-depth analysis of the crackmeter data at Matterhorn (Hasler et al., 2012; Weber et al., 2017).

In the case of the GNSS positions at Matterhorn Hörnligrat all rover positions MH33-MH40, MH43 (the L1-GPS systems) are calculated relative to the two-frequency high-performance GNSS receiver located at MH42/HOGR. However this reference location is also exhibiting significant movement as it is positioned on the top of the buttress between the detachment zone in the second couloir and the first couloir. Therefore the absolute position output of positions MH33-MH40, MH43 contains the movement of the reference position MH42/HOGR. In order to quantify this movement and remove the differences from the rover positions MH33-MH40, MH43 precise absolute positions for MH42/HOGR are calculated using a longer baseline to the non-moving reference station of the Automated GNSS Network of Switzerland (AGNES) operated by swisstopo with station ZERM located at Furi, Zermatt, Switzerland, 1867 m a.s.l. The daily position data series provided with this paper contain the uncorrected position data. Calculating the corrected position values by differencing is straightforward. An example of such corrected data (the relative displacement of the positions MH33-35 and MH42/HOGR) can be seen in Figure 15. Similarly calculating velocities or aggregate displacements using a simple or more complex method (Wirz et al., 2014) is at the discretion of the data user.

6 ~~Examples of~~ Scientific results based on Matterhorn Hörnligrat data~~use~~

Data over the period 2008-2011 were the foundation of A. Hasler's PhD thesis (Hasler, 2011) that investigated the thermal and kinematic regime in steep bedrock permafrost for the first time to this extent and level of detail with important contributions to the spatial variability of the thermal regime (Hasler et al., 2011b) and kinematics (Hasler et al., 2012) ~~nurturing also laboratory experiments (Hasler et al., 2011a). This work was later continued~~ concluding that enhanced movement in summer originates

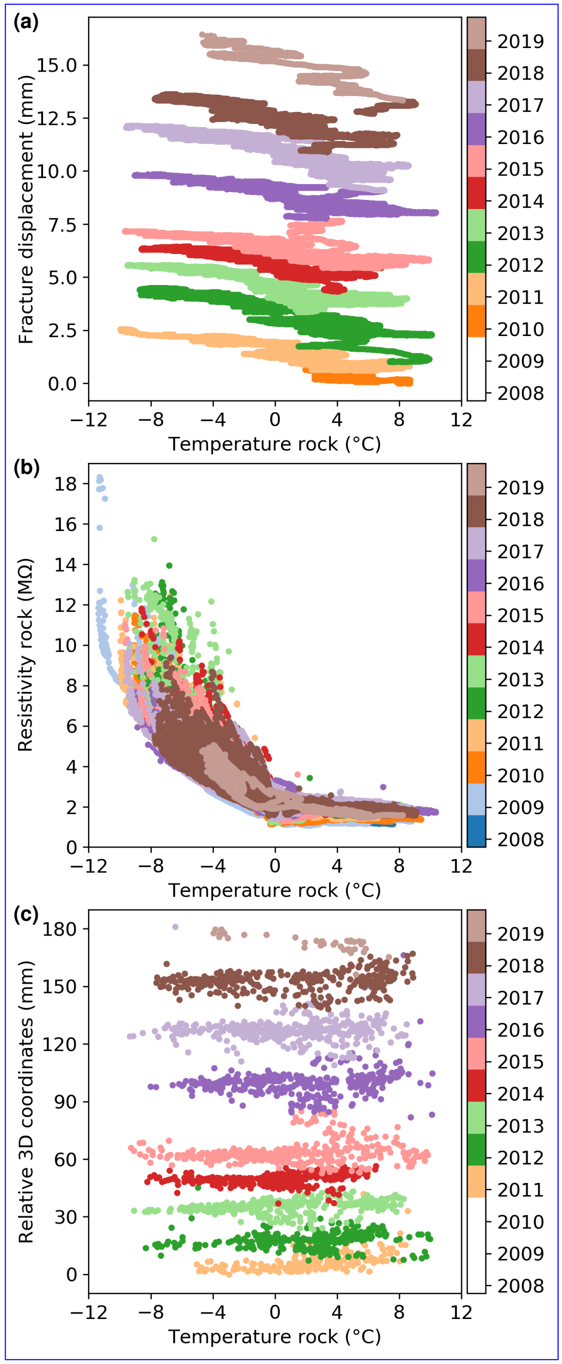

Figure 13. Displacement (~~black~~MH08, dx2)~~and inclination~~, resistivity (~~green~~MH10, 85cm) ~~measured using an L1-GPS sensor for deriving displacement based on daily position data~~ and ~~an integrated 2-axis inclinometer sensor at position MH34~~ relative 3D coordinates derived from L1/L2 GNSS (~~the tower feature in the middle of Fig. ??~~MH42/HOGR) plotted against rock temperature (85cm) at position MH10.

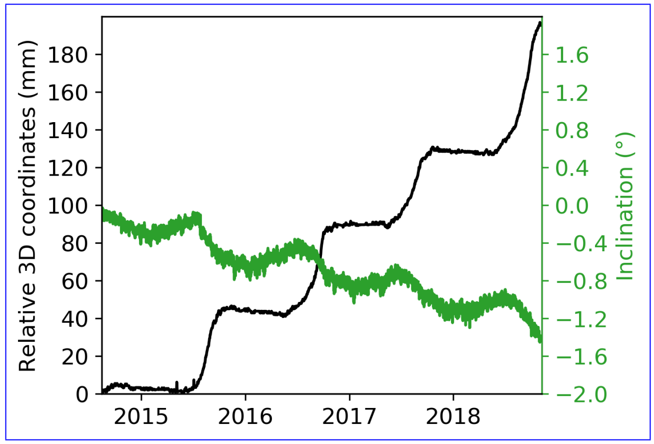

Figure 14. Displacement (black) and inclination (green) measured using an L1-GPS sensor for deriving displacement based on daily position data and an integrated 2-axis inclinometer sensor at position MH34 (the tower feature in the middle of Figure **??**).

from hydro-thermally induced strength reduction in fractures containing perennial ice. This hypothesis was later supported when further data became available over ~~longer monitoring periods~~a longer monitoring period (Weber et al., 2017). Further, in the wider context of rock slope stability assessment, a new metric was proposed to quantify irreversible displacement of fractures based on the statistical separation of reversible components, caused by thermo-elastic strains, from irreversible components due to other processes (Weber et al., 2017). With the addition of acoustic emission and microseismic sensors to the field site S. Weber's PhD Thesis (Weber, 2018) focused more on structural aspects and the characterization of ~~more complex signals~~micro-seismic response to fracture events (Weber et al., 2018c) and on ambient vibrations (Weber et al., 2018b) ~~.~~ with the following major findings: (1) A significant amplification of micro-seismic signals in the frequency band 33 – 67 Hz was found. Filtering in this specific frequency band enables a more reliable detection of fracture events, which is a prerequisite for rock slope stability assessment and early warning. (2) The characterization of the site specific seismic response based on ambient seismic vibration recordings suggests that the temporal variations in resonance frequencies are linked to the formation and melt of ice-fill in bedrock fractures.

Along-side a number of technology-oriented publications have emerged that discuss sensor and wireless network design (Talzi et al., 2007; Hasler et al., 2008; Beutel et al., 2009; Keller et al., 2009b; Buchli et al., 2012; Sutton et al., 2015b, a, 2017a), performance analysis (Keller et al., 2012a, 2011) and smart sensors ~~(Sutton et al., 2017b; ?)~~(Sutton et al., 2017b; Meyer et al., 2019a) . More recently focus has shifted ~~even more to include~~ on even more complex sensing modalities including machine learning methods to the portfolio of application specific data analysis ~~(Meyer et al., 2017; ?)~~(Meyer et al., 2017, 2019b).

~~The data sets published with this paper contain data from the start of measurements on July 25, 2008 until December 31, 2018. Annual updates of this data are planned, but they can also be retrieved by the reader using the toolset described and provided here from our online repository at . An overview of the data availability both for raw primary data and derived data~~

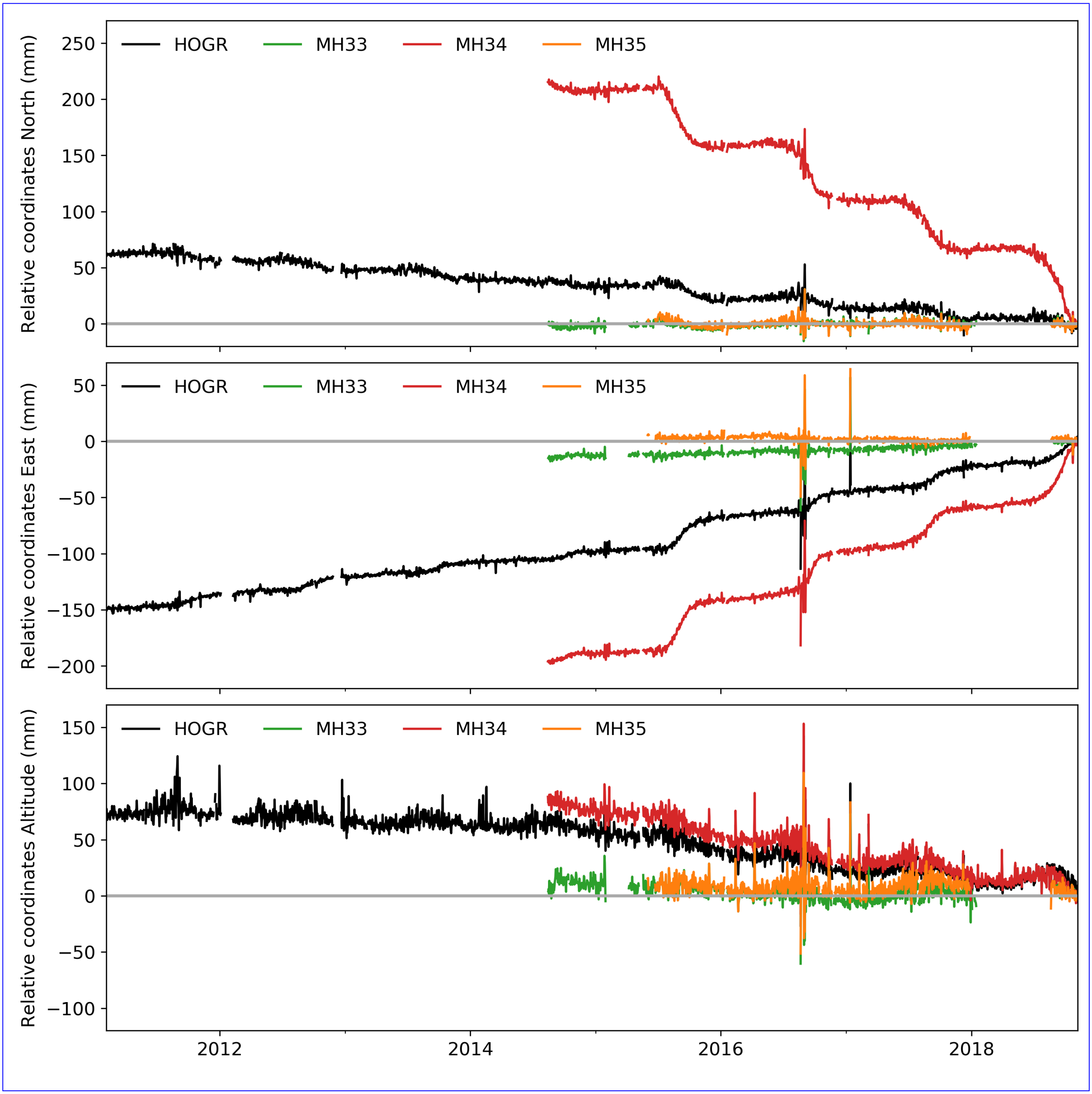

Figure 15. Relative displacement of the GNSS positions measured at Matterhorn Hörnligrat. For an approximate overview of the measurement setting see Figures **??** and **??**.

~~products is given in Figure 6. Since these data sets constitute a large amount of primary data and a large number of data types Table 6 gives a brief overview of the structure, file types and size of the data set.~~

~~Data availability for all data products.~~

7 Code and data availability

The data set (doi.pangaea.de/10.1594/PANGAEA.897640, Weber et al., 2019) published with this paper contains data from the start of measurements on July 25, 2008 until December 31, 2018. An overview on the structure, file types and size of the data sets, both for the raw primary data and derived data products is given in Table 6. Furthermore the data set also contains the key metadata file for the Matterhorn field site: matterhorn_nodeposition.xslx. Annual updates of this data set are planned (living data process). Using the toolset described in Section 5 and using the online repository at http://data.permasense.ch (see Appendix **??** for details) the data user can also create custom updates of the data set independently.

Table 6. Structure, description, formats and sizes of the data set components.

Directory	Data Description	Format	# Data Points	# Files	Size
gnss_data_raw	GNSS raw observations	RINEX 2.11	16’978’024	7’985	27.4 GB
gnss_derived_data_products	daily position data	csv	7’578	48	243.2 MB
timelapse_images	time lapse images	jpg	32’017	32’017	41.5 GB
timeseries_data_raw	raw primary sensor data	csv	94’691’950	395	14.5 GB
timeseries_derived_data_products	sensor data after cleaning/aggregation	csv	2’711’631	361	193.6 MB
timeseries_sanity_plots	standard plots for all data	png	-	223	39.6 MB
matterhorn_nodepositions.xlsx	general metadata file	xlsx	-	1	40 kB
README.md	-	md	-	1	4 kB
Total	-	-	114’421’200	41’031	83.8 GB

~~Furthermore the data set also contains the key metadata file for the Matterhorn field site: `matterhorn_nodeposition.xslx`.~~

The data sets as well as the ~~code~~ toolset (code) for preparing, processing~~and validating~~ , validating and updating the data contained in this publication are available through the following providers and data links:

- Data set
  ~~currently under review with Pangaea~~ https://doi.pangaea.de/10.1594/PANGAEA.897640, (Weber et al., 2019)
- ~~Processing code~~Toolset (processing code)
  https://doi.org/10.5281/zenodo.2542714, (Weber et al., 2019)

8 Conclusion and Outlook

~~The experiments at Matterhorn Hörnligrat and the data sets described in this paper are the results of a truly unique effort. The PermaSense database~~ When reflecting on the past ten+ years of development and operation it is fair to say that the promises of distributed wireless systems have delivered unprecedented detail and quality with respect to data. But on the other side the complexity and requirements for mastering increasing degrees of freedom increased as well. What has been especially troublesome at time was the sheer amount of data. Managing and especially the effort for devising a suitable data management system architecture including implementing workable and sustainable solutions has been greatly underestimated. There are no quick answers, make-or-buy decisions are frequently re-visited and there is no ready-made kitting that can be implemented swiftly. Since we believe that this present publication and it's related data set are already large and complex the acoustic emission and microseismic (AE/MS) data from Matterhorn as well as the terrestrial laserscanning and radar interferometry data are not included although it constitutes an integral part of the observations made at this field site. Parts of the AE/MS data has been published separately as we have indicated earlier, but putting all this into a single publication/data set would have simply been overwhelming.

The PermaSense data set from Matterhorn Hörnligrat is the largest, most fine-grained and diverse data set available for permafrost research worldwide. Remarkable about this data set is not only it's duration but also the diversity and density of measurements. The decade+ of interdisciplinary research summarized here shows in an exemplary way how modern (wireless) technological advancements enable new science and the related breakthroughs. The data described here is multi-facetted, exceptionally rich and therefore constitutes a substantial foundation for further research, e.g. in the area of ~~analysis methodology~~ methodology development, the development of process models, comparative studies, assessment of change in the environment, natural hazard warning and ~~the development of processmodels. Bringing together this data~~ preparing for adaptation. Updates to the data set are planned (living data process) but independent of that the user can obtain updates independently using the toolset provided with this data set. Apart from flexibility, this allows also for maximum transparency and reproducibility of the data presented in this paper.

Opportunities for future work exist in a multitude of ways and we are only highlighting two directions here: Bringing together the data presented in this paper with data from our colleagues in Italy (ARPA VDA, Matterhorn summit, Carrel ridge, Cima Bianche monitoring site) and SLF/WSL + PERMOS (permafrost boreholes on the Swiss side) allows to ~~gain an overview~~ obtain further detail over a large span of ~~different altitude regimes~~ altitude regime of the European Alps as well as ~~north vs. south exposition. Conducting comparative~~ the peculiarities of north- vs. south-facing exposition. Comparative studies to other similar sites, e.g. Aiguille du Midi, Chamonix, France where the altitude and climatic forcing is similar but the morphology and especially the type of rock is very different ~~is~~ are currently ongoing.

~~When reflecting on the past ten+ years of development and operation it is fair to say that the promises of distributed wireless systems have delivered unprecedented detail w.r.t. data . But on the other side the complexity and degrees of freedom increased as well . What has been especially troublesome at time was the sheer amount of data~~

Author contributions. Samuel Weber (SW) and Jan Beutel (JB) prepared the data set and wrote the manuscript with the help of all other authors. The processing code was developed together with Matthias Meyer (MM) and Tonio Gsell (TG). The original PermaSense project was conceived and implemented by Stephan Gruber (SG), Andreas Hasler (AH), Igor Talzi (IT), Christian Tschudin (CT) and Daniel Vonder Mühll (DV) with help from JB. The revised sensor system architecture was designed by JB, Matthias Keller (MK), Roman Lim (RL), Reto Da Forno (RD), TG, Mustafa Yücel (MY) and Lothar Thiele (LT). Alain Geiger (AG) and Philippe Limpach (PL) contributed to the GNSS sensors systems. The data management system was designed by JB, TG, RL, SG, AH, MK, MY and SW, operation was managed by JB, TG, SG, AH, SW, MK, MM and Andreas Vieli (AV).

Competing interests. The authors declare that they have no conflict of interest.

Acknowledgements. The early parts of this work have been funded through the Swiss National Science Foundation National Competence Center on Mobile Information and Communication Systems (NCCR-MICS), the ETH Zurich Competence Center on Environment and Sustainability (CCES) as well as the Swiss Federal Office of the Environment (FOEN) and later through nano-tera.ch, ref. no. 530659. Support in the form of equipment has been given by Hilti Schweiz AG, Arc'teryx and Beal. The technical workshops at ETHZ and UniZH as well as Art of Technology, Zurich contributed to the successful development and implementation of various pieces of equipment. We are indebted to the extraordinary local support we have received for our research activities in Zermatt: ~~Specifically~~ specifically the whole team of Air Zermatt, Kurt Lauber, Stephanie Mayor and the Hörnlihütte team, Alpin Center Zermatt, Kurt Guntli (Zermatter Bergbahnen), Willy Gitz (Sprengtechnik-GFS), Hotel Bahnhof and Serac (Zermatt) as well as the local mountain guides Hermann Biner, Robert Andenmatten, Willy Taugwalder, Urs Lerjen, Benedikt Perren, Bruno Jelk, Hannes Walser, Simon Anthamatten and Anjan Truffer. Without this strong positive welcome this work would not have been possible. Thank you for the trust, confidence and help bestowed by the Swiss ~~federal~~ Federal authorities (Hugo Raetzo, FOEN) and Ct. Valais (Charly Wuilloud, Raphael Mayoraz) into our very special activities on a very special mountain. Martin Vetterli (EPFL) continuously motivated to push hard and think big, ~~Hans-Ueli Gubler (~~Hansueli Gubler (AlpuG, Davos) gave invaluable technical guidance on the first sensor concept, Karl Aberer, Ali Salehi and Sofiane Sarni (EPFL) helped with understanding the GSN data management system, Stephanie Gubler and Nicolas Dawes helped to structure our data, Elmar Brockmann (swisstopo, Wabern) was a regular source of GNSS related answers, Daniel Reinstadler (evoNET, Landeck, Austria) had the perfect solution at hand for transmitting large amounts of data to the Internet that we realized with the help of Maurizio Savina and Paolo Burlando (ETHZ), David Amitrano (Universite Joseph Fourier, Grenoble, France) helped to kick off our work on AE and finally, Philip Deline and Ludovic Ravanel (Universite de Savoie, Chambery) who were courageous enough to trust our technology in order to collaboratively equip Aiguille du Midi (Chamonix, France) with wireless sensors in a similar fashion. Many friends and helpers were involved in field work: Lucas Girard, Lorenz Böckli, Joel Fiddes, Luzia Fischer, Karl Stranski, Vanessa Wirz, Christoph Walser, Raphael Eiter as well as Marcia Phillips, Robert Kenner, Johann Müller (all three TLS) and our colleagues from the "other side" of the mountain: Paolo Pogliotti, Umberto Morra di Cella and Edoardo Cremonese (ARPA VDA, Italy). Last but not least we owe sincere thanks and gratitude to Jeannette Nötzli for tireless consulting concerning permafrost related issues, long-term monitoring strategy, data curation, policy and strategic decisions as well as to Wilfried Häberli for persistent guidance, judicious stewardship and friendship through all the years. Reviews from Paolo Pogliotti, and an anonymous referee provided valuable comments that helped to improve the paper substantially. Finally, we thank the handling Editor Kirsten Elger for constructive feedback and suggestions.

References

Aberer, K., Hauswirth, M., and Salehi, A.: A Middleware for Fast and Flexible Sensor Network Deployment, in: Proceedings of the 32nd International Conference on Very Large Data Bases, VLDB '06, pp. 1199–1202, VLDB Endowment, 2006.

Aberer, K., Alonso, G., Barrenetxea, G., Beutel, J., Bovay, J., Dubois-Ferriere, H., Kossmann, D., Parlange, M., Thiele, L., and Vetterli, M.: Infrastructures for a Smart Earth – The Swiss NCCR-MICS initiative, Praxis der Informationsverarbeitung und Kommunikation, 30, 20–25, https://doi.org/10.1515/PIKO.2007.20, 2007.

Amitrano, D., Gruber, S., and Girard, L.: Evidence of frost-cracking inferred from acoustic emissions in a high-alpine rock-wall, Earth Planet. Sci. Lett., 341–344, 86–93, https://doi.org/10.1016/j.epsl.2012.06.014, 2012.

Beutel, J., Gruber, S., Hasler, A., Lim, R., Meier, A., Plessl, C., Talzi, I., Thiele, L., Tschudin, C., Woehrle, M., and Yuecel, M.: PermaDAQ: A scientific instrument for precision sensing and data recovery in environmental extremes, in: The 8th ACM/IEEE International Conference on Information Processing in Sensor Networks, pp. 265–276, 2009.

Beutel, J., Buchli, B., Ferrari, F., Keller, M., Thiele, L., and Zimmerling, M.: X-Sense: Sensing in Extreme Environments, Proceedings of Design, Automation and Test in Europe (DATE 2011), pp. 1460–1465, https://doi.org/10.1109/DATE.2011.5763236, 2011.

Biskaborn, B. K., Smith, S. L., Noetzli, J., Matthes, H., Vieira, G., Streletskiy, D. A., Schoeneich, P., Romanovsky, V. E., Lewkowicz, A. G., Abramov, A., Allard, M., Boike, J., Cable, W. L., Christiansen, H. H., Delaloye, R., Diekmann, B., Drozdov, D., Etzelmüller, B., Grosse, G., Guglielmin, M., Ingeman-Nielsen, T., Isaksen, K., Ishikawa, M., Johansson, M., Johannsson, H., Joo, A., Kaverin, D., Kholodov, A., Konstantinov, P., Kröger, T., Lambiel, C., Lanckman, J.-P., Luo, D., Malkova, G., Meiklejohn, I., Moskalenko, N., Oliva, M., Phillips, M., Ramos, M., Sannel, A. B. K., Sergeev, D., Seybold, C., Skryabin, P., Vasiliev, A., Wu, Q., Yoshikawa, K., Zheleznyak, M., and Lantuit, H.: Permafrost is warming at a global scale, Nature Communications, 10, https://doi.org/10.1038/s41467-018-08240-4, 2019.

Bucher, K., Dal Piaz, G. V., Oberhänsli, R., Gouffon, Y., Martinotti, G., and Polino, R.: Blatt 1347 Matterhorn. Geol. Atlas Schweiz 1:25 000, Erläut. 107, Bundesamt für Wasser und Geologie, Wabern, 2004.

Buchli, B., Sutton, F., and Beutel, J.: GPS-equipped Wireless Sensor Network Node for High-accuracy Positioning Applications, Lecture Notes on Computer Science 7158. Proc. of 9th European Conference on Wireless Sensor Networks (EWSN 2012), pp. 179–195, 2012.

Burri, N., von Rickenbach, P., and Wattenhofer, R.: Dozer: Ultra-Low Power Data Gathering in Sensor Networks, in: 6th International Symposium on Information Processing in Sensor Networks, pp. 450–459, https://doi.org/10.1109/IPSN.2007.4379705, 2007.

Caduff, R., Schlunegger, F., Kos, A., and Wiesmann, A.: A review of terrestrial radar interferometry for measuring surface change in the geosciences, Earth Surface Processes and Landforms, 40, 208–228, https://doi.org/10.1002/esp.3656, 2015.

Coviello, V., Chiarle, M., Arattano, M., Pogliotti, P., and di Cella, U. M.: Monitoring Rock Wall Temperatures and Microseismic Activity for Slope Stability Investigation at J.A. Carrel Hut, Matterhorn, in: Engineering Geology for Society and Territory - Volume 1, edited by Lollino, G., Manconi, A., Clague, J., Shan, W., and Chiarle, M., pp. 305–309, Springer International Publishing, Cham, 2015.

Dach, R., Lutz, S., Walser, P., and Fridez, P.: Bernese GNSS Software Version 5.2. User manual, Astronomical Institute, University of Bern, https://doi.org/10.7892/boris.72297, 2015.

Daily, W., Ramirez, A., Binley, A., and LaBrecque, D.: 17. Electrical Resistance Tomography—Theory and Practice, pp. 525–550, Society of Exploration Geophysicists, https://doi.org/10.1190/1.9781560801719.ch17, 2012.

Davies, M., Hamza, O., and Harris, C.: The effect of rise in mean annual temperature on the stability of rock slopes containing ice-filled discontinuities, Permafrost and Periglacial Process., 12, 137–144, https://doi.org/0.1002/ppp 378, 2001.

Draebing, D., Krautblatter, M., and Hoffmann, T.: Thermo-cryogenic controls of fracture kinematics in permafrost rockwalls, Geophysical Research Letters, 44, 3535–3544, https://doi.org/10.1002/2016GL072050, 2017.

Faillettaz, J., Funk, M., and Vagliasindi, M.: Time forecast of a break-off event from a hanging glacier, The Cryosphere, 10, 1191–1200, https://doi.org/10.5194/tc-10-1191-2016, 2016.

Fischer, L., Kääb, A., Huggel, C., and Noetzli, J.: Geology, glacier retreat and permafrost degradation as controlling factors of slope instabilities in a high-mountain rock wall: the Monte Rosa east face, Natural Hazards and Earth System Sciences, 6, 761–772, https://doi.org/10.5194/nhess-6-761-2006, 2006.

Fort, M., Cossart, E., Deline, P., Dzikowski, M., Nicoud, G., Ravanel, L., Schoeneich, P., and Wassmer, P.: Geomorphic impacts of large and rapid mass movements: a review, Geomorphologie: relief, processus, environnement, 15, 47–64, https://doi.org/10.4000/geomorphologie.7495, 2009.

Girard, L., Beutel, J., Gruber, S., Hunziker, J., Lim, R., and Weber, S.: A custom acoustic emission monitoring system for harsh environments: Application to freezing-induced damage in alpine rock walls, Geosci. Instrum. Method. Data Syst., 1, 155–167, https://doi.org/10.5194/gi-1-155-2012, 2012.

Girard, L., Gruber, S., Weber, S., and Beutel, J.: Environmental controls of frost cracking revealed through in-situ acoustic emission measurements in steep bedrock, Geophys. Res. Lett., 40, 1748–1753, https://doi.org/10.1002/grl.50384, 2013.

Gischig, S., Moore, J. R., Evans, K. F., Amann, F., and Loew, S.: Thermomechanical forcing of deep rock slope deformation: 2. The Randa rock slope instability, Journal of Geophysical Research: Earth Surface, 116, https://doi.org/10.1029/2011JF002007, 2011.

Gobiet, A., Kotlarski, S., Beniston, M., Heinrich, G., Rajczak, J., and Stoffel, M.: 21st century climate change in the European Alps—A review, Science of The Total Environment, 493, 1138 – 1151, https://doi.org/https://doi.org/10.1016/j.scitotenv.2013.07.050, 2014.

Gruber, S. and Haeberli, W.: Permafrost in steep bedrock slopes and its temperature-related destabilization following climate change, J. Geophys. Res., 112, F02S18, https://doi.org/10.1029/2006JF000547, 2007.

Gruber, S., Peter, M., Hoelzle, M., Woodhatch, I., and Haeberli, W.: Surface temperatures in steep Alpine rock faces - a strategy for regional-scale measurement and modelling, in: Proceedings of the 8th International Conference on Permafrost 2008, Zurich, Switzerland, vol. 1, pp. 325–330, 2003.

Gruber, S., Hoelzle, M., and Haeberli, W.: Permafrost thaw and destabilization of Alpine rock walls in the hot summer of 2003, Geophys. Res. Lett., 31, L13 504, https://doi.org/10.1029/2004GL020051, 2004a.

Gruber, S., Hoelzle, M., and Haeberli, W.: Rock-wall temperatures in the Alps: modelling their topographic distribution and regional differences, Permafrost and Periglacial Processes, 15, 299–307, https://doi.org/10.1002/ppp.501, 2004b.

Gruber, S., King, L., Kohl, T., Herz, T., Haeberli, W., and Hoelzle, M.: Interpretation of geothermal profiles perturbed by topography: the alpine permafrost boreholes at Stockhorn Plateau, Switzerland, Permafrost and Periglacial Processes, 15, 349–357, https://doi.org/10.1002/ppp.503, https://onlinelibrary.wiley.com/doi/abs/10.1002/ppp.503, 2004c.

Gruber, S., Burn, C., Arenson, L., Geertsema, M., Harris, S., Smith, S., Bonnaventure, P., and Benkert, B.: Permafrost in mountainous regions of Canada, in: Proc. 68th Canadian Geotechnical Conference, 7th Canadian Permafrost Conference, Canadian Geotechnical Society, Québec-City, Qc, Canada, 2015.

Gruber, S., Fleiner, R., Guegan, E., Panday, P., Schmid, M.-O., Stumm, D., Wester, P., Zhang, Y., and Zhao, L.: Review article: Inferring permafrost and permafrost thaw in the mountains of the Hindu Kush Himalaya region, The Cryosphere, 11, 81–99, https://doi.org/10.5194/tc-11-81-2017, https://www.the-cryosphere.net/11/81/2017/, 2017.

Günzel, F.: Shear strength of ice-filled rock joints, in: Proceedings of the 9th International Conference on Permafrost, edited by Hinkel, K. M., vol. 1, p. 581–586, 2008.

Haeberli, W., Noetzli, J., and Springman, S.: Matterhorn „for ever“?, in: Matterhorn – Berg der Berge, edited by Anker, D., pp. 294–301, AS Verlag & Buchkonzept, Zürich, 2015.

Haeberli, W., Schaub, Y., and Huggel, C.: Increasing risks related to landslides from degrading permafrost into new lakes in de-glaciating mountain ranges, Geomorphology, 293, 405 – 417, https://doi.org/10.1016/j.geomorph.2016.02.009, 2017.

Hall, K., Thorn, C. E., Matsuoka, N., and Prick, A.: Weathering in cold regions: Some thoughts and perspectives, Prog. Phys. Geogr., 26, 577–603, https://doi.org/10.1191/0309133302pp353ra, 2002.

Hasler, A.: Thermal conditions and kinematics of steep bedrock permafrost, Ph.D. thesis, University of Zurich, 2011.

Hasler, A., Talzi, I., Beutel, J., Tschudin, C., and Gruber, S.: Wireless sensor networks in permafrost research: Concept, requirements, implementation, and challenges, in: Proceedings of the 9th International Conference on Permafrost, 2008.

Hasler, A., Gruber, S., Font, M., and Dubois, A.: Advective heat transport in frozen rock clefts: Conceptual model, laboratory experiments and numerical simulation, Permafrost and Periglacial Process., 22, 378–389, https://doi.org/10.1002/ ppp.737, 2011a.

Hasler, A., Gruber, S., and Haeberli, W.: Temperature variability and offset in steep alpine rock and ice faces, The Cryosphere, 5, 977–988, https://doi.org/10.5194/tc-5-977-2011, 2011b.

Hasler, A., Gruber, S., and Beutel, J.: Kinematics of steep bedrock permafrost, J. Geophys. Res., 117, F01 016, https://doi.org/10.1029/2011JF001981, 2012.

Hiebl, J., Auer, I., Böhm, R., Schöner, W., Maugeri, M., Lentini, G., Spinoni, J., Brunetti, M., Nanni, T., Tadić, M., Pervcec Bihari, Z., Dolinar, M., and Müller-Westermeier, G.: A high-resolution 19611990 monthly temperature climatology for the greater Alpine region, Meteorologische Zeitschrift, 18, 507–530, https://doi.org/10.1127/0941-2948/2009/0403, http://dx.doi.org/10.1127/0941-2948/2009/0403, 2009.

Huggel, C., Zgraggen-Oswald, S., Haeberli, W., Kääb, A., Polkvoj, A., Galushkin, I., and Evans, S. G.: The 2002 rock/ice avalanche at Kolka/Karmadon, Russian Caucasus: Assessment of extraordinary avalanche formation and mobility, and application of QuickBird satellite imagery, Natural Hazards and Earth System Sciences, 5, 173–187, https://doi.org/10.5194/nhess-5-173-2005, 2005.

Huggel, C., Allen, S., Deline, P., Fischer, L., Noetzli, J., and Ravanel, L.: Ice thawing, mountains falling—are alpine rock slope failures increasing?, Geology Today, 28, 98–104, https://doi.org/10.1111/j.1365-2451.2012.00836.x, 2012.

Hurter, F., Geiger, A., Perler, D., and Rothacher, M.: GNSS water vapor monitoring in the Swiss Alps, in: 2012 IEEE International Geoscience and Remote Sensing Symposium, pp. 1972–1975, https://doi.org/10.1109/IGARSS.2012.6351115, 2012.

Jia, H., Xiang, W., and Krautblatter, M.: Quantifying rock fatigue and decreasing compressive and tensile strength after repeated freeze-thaw cycles, Permafrost and Periglacial Process., 26, 368–377, https://doi.org/10.1002/ppp.1857, 2015.

Keller, M., Beutel, J., and Thiele, L.: Mountainview - Precision Image Sensing on High-Alpine Locations, in: Proc. 6th European Conference on Sensor Networks (EWSN 2009), pp. 15–16, Springer, Cork, Ireland, 2009a.

Keller, M., Yuecel, M., and Beutel, J.: High Resolution Imaging for Environmental Monitoring Applications, in: International Snow Science Workshop 2009: Programme and Abstracts, pp. 197–201, Davos, Switzerland, 2009b.

Keller, M., Woehrle, M., Lim, R., Beutel, J., and Thiele, L.: Comparative performance analysis of the PermaDozer protocol in diverse deployments, in: 2011 IEEE 36th Conference on Local Computer Networks, pp. 957–965, https://doi.org/10.1109/LCN.2011.6115578, 2011.

Keller, M., Beutel, J., Saukh, O., and Thiele, L.: Visualizing large sensor network data sets in space and time with vizzly, in: 37th Annual IEEE Conference on Local Computer Networks - Workshops, pp. 925–933, https://doi.org/10.1109/LCNW.2012.6424084, 2012a.

Keller, M., Beutel, J., and Thiele, L.: How Was Your Journey?: Uncovering Routing Dynamics in Deployed Sensor Networks with Multi-hop Network Tomography, in: Proceedings of the 10th ACM Conference on Embedded Network Sensor Systems, SenSys '12, pp. 15–28, ACM, New York, NY, USA, https://doi.org/10.1145/2426656.2426659, 2012b.

Keuschnig, M., Krautblatter, M., Hartmeyer, I., Fuss, C., and Schrott, L.: Automated Electrical Resistivity Tomography Testing for Early Warning in Unstable Permafrost Rock Walls Around Alpine Infrastructure, Permafrost and Periglacial Processes, 28, 158–171, https://doi.org/10.1002/ppp.1916, 2017.

Krautblatter, M.: Detection and quantification of permafrost change in alpine rock walls and implications for rock instability, Ph.D. thesis, Bonn University, 2009.

Krautblatter, M. and Hauck, C.: Electrical resistivity tomography monitoring of permafrost in solid rock walls, Journal of Geophysical Research: Earth Surface, 112, F02S20, https://doi.org/10.1029/2006JF000546, 2007.

Krautblatter, M., Funk, D., and Günzel, F.: Why permafrost rocks become unstable: A rock-ice-mechanical model in time and space, Earth Surf. Process. Landf., 38, 876–887, https://doi.org/10.1002/esp.3374, 2013.

Levis, P., Madden, S., Polastre, J., Szewczyk, R., Whitehouse, K., Woo, A., Gay, D., Hill, J., Welsh, M., Brewer, E., and Culler, D.: TinyOS: An Operating System for Sensor Networks, pp. 115–148, Springer Berlin Heidelberg, Berlin, Heidelberg, https://doi.org/10.1007/3-540-27139-2_7, 2005.

Luethi, R. and Phillips, M.: Challenges and solutions for long-term permafrost borehole temperature monitoring and data interpretation, Geographica Helvetica, 71, 121–131, https://doi.org/10.5194/gh-71-121-2016, 2016.

Magnin, F., Deline, P., Ravanel, L., Noetzli, J., and Pogliotti, P.: Thermal characteristics of permafrost in the steep alpine rock walls of the Aiguille du Midi (Mont Blanc Massif, 3842 m a.s.l), The Cryosphere, 9, 109–121, https://doi.org/10.5194/tc-9-109-2015, 2015.

Mamot, P., Weber, S., Schröder, T., and Krautblatter, M.: A temperature- and stress-controlled failure criterion for ice-filled permafrost rock joints, The Cryosphere Discussions, 2018, 1–31, https://doi.org/10.5194/tc-2018-57, accepted for publication in The Cryosphere, 2018.

Matsuoka, N. and Murton, J.: Frost weathering: Recent advances and future directions, Permafrost and Periglacial Process., 19, 195–210, https://doi.org/10.1002/ppp.620, 2008.

Mellor, M.: Mechanical properties of rocks at low temperatures, in: 2nd International Conference on Permafrost, Yakutsk, pp. 334–344, International Permafrost Association, 1973.

MeteoSwiss: Climate normals from all measuring stations with long-time series of measurements, https://www.meteoswiss.admin.ch/home/climate/swiss-climate-in-detail/climate-normals/normal-values-per-measured-parameter.html, 2019.

Meyer, M., Beutel, J., and Thiele, L.: Unsupervised feature learning for audio analysis, in: Workshop track - ICLR 2017, 2017.

Meyer, M., Weber, S., Beutel, J., Gruber, S., Gsell, T., Hasler, A., and Vieli, A.: Micro-Seismic And Image Dataset Acquired At Matterhorn Hörnligrat, Switzerland, https://doi.org/10.5281/zenodo.1320834, 2018.

Meyer, M., Farei-Campagna, T., Pasztor, A., Forno, R. D., Gsell, T., Faillettaz, J., Vieli, A., Weber, S., Beutel, J., and Thiele, L.: Event-triggered Natural Hazard Monitoring with Convolutional Neural Networks on the Edge, in: Proceedings of the 18th International Conference on Information Processing in Sensor Networks, IPSN '19, pp. 73–84, ACM, New York, NY, USA, https://doi.org/10.1145/3302506.3310390, 2019a.

Meyer, M., Weber, S., Beutel, J., and Thiele, L.: Systematic identification of external influences in multi-year microseismic recordings using convolutional neural networks, Earth Surface Dynamics, 7, 171–190, https://doi.org/10.5194/esurf-7-171-2019, https://www.earth-surf-dynam.net/7/171/2019/, 2019b.

Murton, J., Peterson, R., and Ozouf, J.-C.: Bedrock fracture by ice segregation in cold regions, Science, 314, 1127–1129, https://doi.org/10.1126/science.1132127, 2006.

Noetzli, J., Gruber, S., Kohl, T., Salzmann, N., and Haeberli, W.: Three-dimensional distribution and evolution of permafrost temperatures in idealized high-mountain topography, Journal of Geophysical Research: Earth Surface, 112, https://doi.org/10.1029/2006JF000545, 2007.

Noetzli, J., Christiansen, H., Deline, P., Gugliemin, M., Isaksen, K., Romanovsky, V., Smith, S., Zhao, L., and Streletskiy, D. A.: Permafrost thermal state, in: State of the Climate in 2017, 99, pp. S20–S22, Bulletin of the American Meteorological Society, https://doi.org/10.1175/2018BAMSStateoftheClimate.1, 2018.

Noetzli, J., Pellet, C., and Staub, B., eds.: PERMOS 2019. Permafrost in Switzerland 2014/2015 to 2017/2018, Glaciological Report (Permafrost) No. 16-19 of the Cryospheric Commission of the Swiss Academy of Sciences (SCNAT), https://doi.org/10.13093/permos-rep-2019-16-19, 2019.

Occhiena, C., Coviello, V., Arattano, M., Chiarle, M., Morra di Cella, U., Pirulli, M., Pogliotti, P., and Scavia, C.: Analysis of microseismic signals and temperature recordings for rock slope stability investigations in high mountain areas, Nat. Hazards Earth Syst. Sci., 12, 2283–2298, https://doi.org/10.5194/nhess-12-2283-2012, 2012.

PERMOS Database 2019: Swiss Permafrost Monitoring Network (PERMOS), https://doi.org/10.13093/permos-2019-01, 2019.

Pogliotti, P., Guglielmin, M., Cremonese, E., Morra di Cella, U., Filippa, G., Pellet, C., and Hauck, C.: Warming permafrost and active layer variability at Cime Bianche, Western European Alps, The Cryosphere, 9, 647–661, https://doi.org/10.5194/tc-9-647-2015, 2015.

Popescu, R.: Permafrost investigations in Iezer Mountains, Southern Carpathians, Revista de Geomorfologie, 20, 102–122, https://doi.org/10.21094/rg.2018.033, 2018.

Ravanel, L. and Deline, P.: Climate influence on rockfalls in high-Alpine steep rockwalls: The north side of the Aiguilles de Chamonix (Mont Blanc massif) since the end of the 'Little Ice Age', The Holocene, 21, 357–365, https://doi.org/10.1177/0959683610374887, 2011.

Ravanel, L. and Deline, P.: Rockfall hazard in the Mont Blanc massif increased by the current atmospheric warming, in: IAEG 12th Congress, edited by Lollino, G., Manconi, A., Clague, J., Shan, W., and Chiarle, M., Climate Change and Engineering Geology, pp. p. 425–428, Torino, Italy, https://hal-sde.archives-ouvertes.fr/hal-01896005, 2014.

Ravanel, L., Allignol, F., Deline, P., Gruber, S., and Ravello, M.: Rock falls in the Mont Blanc Massif in 2007 and 2008, Landslides, 7, 493–501, https://doi.org/10.1007/s10346-010-0206-z, 2010.

Ravanel, L., Magnin, F., and Deline, P.: Impacts of the 2003 and 2015 summer heatwaves on permafrost-affected rock-walls in the Mont Blanc massif, Science of The Total Environment, 609, 132 – 143, https://doi.org/https://doi.org/10.1016/j.scitotenv.2017.07.055, 2017.

Sass, O.: Rock moisture fluctuations during freeze-thaw cycles: Preliminary results from electrical resistivity measurements, Polar Geography, 28, 13–31, https://doi.org/10.1080/789610157, 2004.

Sass, O.: Rock moisture measurements: Techniques, results, and implications for weathering, Earth Surface Processes and Landforms, 30, 359–374, https://doi.org/10.1002/esp.1214, 2005.

Sutton, F., Buchli, B., Beutel, J., and Thiele, L.: Zippy: On-Demand Network Flooding, in: Proceedings of the 13th ACM Conference on Embedded Networked Sensor Systems, SenSys '15, pp. 45–58, ACM, New York, NY, USA, https://doi.org/10.1145/2809695.2809705, 2015a.

Sutton, F., Zimmerling, M., Da Forno, R., Lim, R., Gsell, T., Giannopoulou, G., Ferrari, F., Beutel, J., and Thiele, L.: Bolt: A Stateful Processor Interconnect, in: Proceedings of the 13th ACM Conference on Embedded Networked Sensor Systems, SenSys '15, pp. 267–280, ACM, New York, NY, USA, https://doi.org/10.1145/2809695.2809706, 2015b.

Sutton, F., Da Forno, R., Beutel, J., and Thiele, L.: BLITZ: A Network Architecture for Low Latency and Energy-efficient Event-triggered Wireless Communication, in: Proceedings of the 4th ACM Workshop on Hot Topics in Wireless, HotWireless '17, pp. 55–59, ACM, New York, NY, USA, https://doi.org/10.1145/3127882.3127883, 2017a.

Sutton, F., Da Forno, R., Gschwend, D., Gsell, T., Lim, R., Beutel, J., and Thiele, L.: The Design of a Responsive and Energy-efficient Event-triggered Wireless Sensing System, in: Proceedings of the 2017 International Conference on Embedded Wireless Systems and Networks, EWSN 2017, pp. 144–155, Junction Publishing, USA, http://dl.acm.org/citation.cfm?id=3108009.3108028, 2017b.

Talzi, I., Hasler, A., Gruber, S., and Tschudin, C.: PermaSense: Investigating Permafrost with a WSN in the Swiss Alps, in: Proceedings of the 4th Workshop on Embedded Networked Sensors, EmNets '07, pp. 8–12, ACM, New York, NY, USA, https://doi.org/10.1145/1278972.1278974, 2007.

Teunissen, P. J. and Montenbruck, O., eds.: Handbook of Global Navigation Satellite Systems, Springer International Publishing, https://doi.org/10.1007/978-3-319-42928-1, 2017.

Tomoji, T.: RTKLIB: An Open Source Program Package for GNSS Positioning, http://www.rtklib.com, 2018.

Walder, J. and Hallet, B.: A theoretical model of the fracture of rock during freezing, Geological Society of America Bulletin, 96, 336–346, https://doi.org/10.1130/0016-7606(1985)96<336:ATMOTF>2.0.CO;2, 1985.

Weber, S.: Rock Slope Dynamics in Bedrock Permafrost: Insights Across Scales, Ph.D. thesis, University of Zurich, 2018.

Weber, S., Gruber, S., Girard, L., and Beutel, J.: Design of a measurement assembly to study in situ rock damage driven by freezing, in: Proceedings of the 10th Interntational Conference on Permafrost, Salekhard, Russia, edited by Hinkel, K. M., vol. 1, pp. 437–442, 2012.

Weber, S., Beutel, J., Faillettaz, J., Hasler, A., Krautblatter, M., and Vieli, A.: Quantifying irreversible movement in steep, fractured bedrock permafrost on Matterhorn (CH), The Cryosphere, 11, 567–583, https://doi.org/10.5194/tc-11-567-2017, 2017.

Weber, S., Beutel, J., Gruber, S., Gsell, T., Hasler, A., and Vieli, A.: Rock-temperature, fracture displacement and acoustic/micro-seismic data measured at Matterhorn Hörnligrat, Switzerland, https://doi.org/10.5281/zenodo.1163037, 2018a.

Weber, S., Fäh, D., Beutel, J., Faillettaz, J., Gruber, S., and Vieli, A.: Ambient seismic vibrations in steep bedrock permafrost used to infer variations of ice-fill in fractures, Earth and Planetary Science Letters, 501, 119–127, https://doi.org/10.1016/j.epsl.2018.08.042, 2018b.

Weber, S., Faillettaz, J., Meyer, M., Beutel, J., and Vieli, A.: Acoustic and micro-seismic characterization in steep bedrock permafrost on Matterhorn (CH), Journal of Geophysical Research: Earth Surface, 123, 1363–1385, https://doi.org/10.1029/2018JF004615, 2018c.

Weber, S., Beutel, J., Da Forno, R., Geiger, A., Gruber, S., Gsell, T., Hasler, A., Keller, M., Lim, R., Limpach, P., Meyer, M., Talzi, I., Thiele, L., Tschudin, C., Vieli, A., Vonder Mühll, D., and Yücel, M.: In-situ measurements in steep bedrock permafrost in an Alpine environment on the Matterhorn Hörnligrat, Zermatt Switzerland, https://doi.org/10.1594/PANGAEA.897640, https://doi.org/10.1594/PANGAEA.897640, supplement to: Weber, S et al. (submitted): A decade of detailed observations (2008-2018) in steep bedrock permafrost at Matterhorn Hörnligrat (Zermatt, CH). Earth System Science Data, 2019.

Weber, S., Beutel, J., and Meyer, M.: Code for PermaSense GSN data management, https://doi.org/10.5281/zenodo.2542714, 2019.

Wegmann, M.: Permafrost in bedrock, in: Mountain permafrost and slope stability in the periglacial belt of the Alps. Proceedings of VIth International Conference on Geomorphology, Bologna, edited by Dramis, F., pp. 47–51, 1997.

Wegmann, M.: Frostdynamik in hochalpinen Felswänden am Beispiel der Region Jungfraujoch-Aletsch, Ph.D. thesis, VAW, ETH Zürich, Switzerland, 1998.

Westoby, M., Glasser, N., Brasington, J., Hambrey, M., Quincey, D., and Reynolds, J.: Modelling outburst floods from moraine-dammed glacial lakes, Earth-Science Reviews, 134, 137 – 159, https://doi.org/10.1016/j.earscirev.2014.03.009, 2014.

Wirz, V., Beutel, J., Buchli, B., Gruber, S., and Limpach, P.: Temporal Characteristics of Different Cryosphere-Related Slope Movements in High Mountains, pp. 383–390, Springer, Berlin, Heidelberg, https://doi.org/10.1007/978-3-642-31337-0_49, 2013.

Wirz, V., Beutel, J., Gruber, S., Gubler, S., and Purves, R. S.: Estimating velocity from noisy GPS data for investigating the temporal variability of slope movements, Natural Hazards and Earth System Sciences, 14, 2503–2520, https://doi.org/10.5194/nhess-14-2503-2014, 2014.

Zhao, L., Wu, Q., Marchenko, S., and Sharkhuu, N.: Thermal state of permafrost and active layer in Central Asia during the international polar year, Permafrost and Periglacial Processes, 21, 198–207, https://doi.org/10.1002/ppp.688, 2010.